UNIVERSITY OF TARTU

FACULTY OF SCIENCE AND TEHCNOLOGY

INSTITUE OF MOLECULAR AND CELL BIOLOGY

CHAIR OF DEVELOPMENTAL BIOLOGY

The role of β-integrin *myospheroid* in the wing development of *Drosophila melanogaster*

Master's thesis in gene technology

30 EAP

Marko Leevik

Supervisors: Professor Osamu Shimmi

PhD Tambet Tõnissoo

TARTU 2020

Info page

The role of β-integrin *myospheroid* in the wing development of *Drosophila melanogaster*

Integrins are family of transmembrane cell adhesion receptors that are very important organism development. Integrins are responsible for many cellular function including proliferation, migration, polarisation, apoptosis and differentiation. Integrins are composed from two subunits α and β. To study the spatiotemporal importance of β-integrin to wing phenotype of *Drosophila melanogaster*, UAS/GAL4 system under control of thermosensitive GAL80 system was used was used in this thesis.

CERCS: B350 Development biology, growth (animal), ontogeny, embryology

Key words: *Drosophila melanogaster*, integrin, Myospheroid (Mys)

β-integriini myospheroid roll äädikakärbse *Drosophila melanogaster*-i tiiva arengus

Integriinid, kuuludes transmebraansete raku adhesiooniretseptorvalkude perekonda, omavad olulist rolli organimi arengus. Integriinid vastutavad mitmete rakuliste funktsioonide eest, näiteks proliferatioon, migratsioon, polarisatsioon ning diferentsioon. Integriinid koosnevad kahest subühikust:α-st ning β-st. Uurimaks β-integriini aegruumilist olulisust *Drosophila melanogaster*-i tiiva fenotüübile, kasutati UAS/GAL4 süsteemi, mis oli temperatuuritundliku GAL80 süsteemi kontrolli all.

CERCS: B350 Arengubioloogia, loomade kasv, ontogenees, embrüoloogia

Märksõnad: *Drosophila melanogaster*, integriin, Myospheroid (Mys)

Table of contents

Abbreviations

Ap – Apterous

A/P – anterior-posterior axis

AP – after pupariation

APF – after puparium formation

BMP – Bone morphogenetic proteins

BPF – before puparium formation

CA – constitutively active

Dl – Delta

D. melanogaster – Drosophila melanogaster

DN – dominant negative

DP – disc proper

Dpp – Decapentaplegic

D/V – dorsal-ventral axis

EC – endothelial cell

ECM – extracellular matrix

Egfr – Epidermal growth factor receptor

En – Engrailed

Hh – Hedgehog

Mys – *Myospheroid*

UAS – Upstream activation sequence

PE – peripodial epithelium

P/D – proximal-distal axis

SD – standard deviation

Ser – Serrate

Wg – Wingless

WT – wild type

YW – yellow-white

20HE – 20-hydroxyecdysone

Introduction

Although functioning of organism has been thoroughly studied, new scientific discoveries raise more new questions. With the development of scientific technology, discoveries that initially seemed to be completed are now reconsidered and on the most fundamental processes.

Organisms consist of cells. Integrins that acting like "hands" of the cell are the primary receptors for the extracellular matrix (ECM). These proteins situate in the cell membrane and connect ECM to the actin cytoskeleton. Integrins are mediating multiple essential functions and signaling systems in the living organism, for instance regulation of the cell cycle, organization of the intracellular cytoskeleton and one such example is evolutionarily conserved signaling protein Bone Morphogenetic Protein (BMP). BMPs are highly conserved in multiple species. For instance, *Drosophila melanogaster* equivalent for BMP is Decapentaplegic (Dpp) which is orthologue to human BMP2 and BMP4. BMP signaling is necessary for directing tissue size control, cell differentiation and proliferation. According to this, organism develops constantly.

The aim of this thesis is to describe spatiotemporal effect of β-integrin Myospheroid on the wing morphogenesis of **fruit fly** *Drosophila melanogaster* and find connections with Dpp signaling system using UAS/GAL4 system together with temperature sensitive GAL80 system.

Experiments of this thesis are made in the University of Helsinki in professor Osamu Shimmi's laboratory.

1. Literature overview

1.1. *Drosophila melanogaster* as a model organism

Insects have been used as very important model in many areas of biology. Especially, the fruit fly, *D. melanogaster*, belonging to the order of *Diptera* and the family of *Drosophilidae*, have been an attractive and effective genetic model organism more than one hundred years since American geneticist Thomas Hunt Morgan made heredity discoveries with them. As a result of his work, *D. melanogaster* became widespread model organism in genetics, but additionally served as important model systems in cell, molecular, developmental and neurobiology and behavioral tests. Today, it is one of the best characterized model organisms. Development of considerable number of techniques and experimental systems makes the *D. melanogaster* one of the best model organism for genetic analyses. (Adams *et al*., 2000; Friedman and Hughes, 2001)

There are plenty of advantages for using the *D. melanogaster* as an effective model organism: short generation time (approximately 10 days), relatively cheap, easily cultured and maintained in laboratories, large number of offspring (female fly can lay up to 50-70 eggs per day) and they have compact genome which can be easily manipulate genetically. Even though the common ancestor of flies and vertebrates is traced back at the Protostome-Deuterostome split 700 million years ago, a lot of developmental processes and signaling pathways are highly conserved. (Adams *et al*., 2000; Arias *et al*., 2008). Many of the genes in *D. melanogaster* have clear homologues in higher eukaryotes, for instance *Homo sapiens*. Due to genetic screenings it is possible to identify genes necessary for a particular process and discover specific functions of different genes (St Johnston, 2002). Article from 2000 "A Survey of Human Disease Gene Counterparts in the Drosophila Genome" by Mark E. Fortini claims that 62% of human disease genes were found to have likely homologues in *D. melanogaster* (Fortini *et al*., 2000). Therefore, it can be assumed that *D. melanogaster* provides powerful system as a model for studying human diseases, including cancer, neurological diseases and metabolic disorders. In addition, approval by animal welfare ethical review boards is not necessary for applying experiments to *D. melanogaster* which provides advantage compared, for instance rodents (Festing and Wilkinson, 2007).

1.2. Life cycle of *Drosophila melanogaster*

D. melanogaster is a holometabolous insect that undergoes a full metamorphosis with a distinct four stages and lasts approximately 9-10 days at 25ºC. The life cycle starts with a fertilized egg that is laid on the food in culture jar. In a fertilized egg, embryogenesis takes place. The embryonic development lasts about one day, succeeded by hatching into the first instar larva. The *D. melanogaster* has three distinct instar stages which are separated by molting. The main purpose at larva stages for fruit fly is collecting nutrients and gains size. The first instar larva feeds on the medium that the eggs were laid in and after 25 hours it molts into the second instar larva. Approximately 24 hours later, the second instar larva molts into the third instar larva. Third instar larva starts to climb upwards out of food to a dry and clean place searching for a place to pupariate for 24–48 hours. Third instar larva stops moving, the cuticle hardens and darkens progressively – puparium is formed. 4 hours after puparium formation prepupal molt and after 12 hours pupation takes place. During the pupal stage, which lasts for 3,5-4,5 days, the *D. melanogaster* is metamorphosing into the adult fly, also called as *imago*. In this process, most of larval structures are restructured (Malphigian tubules, fat bodies, gonads) or lysed and adult structures are formed from histoblasts and imaginal discs. These are mitotic within the larva throughout instar stages. Histoblasts are forming abdominal epidermis and internal organs while imaginal discs will form epidermal structures, such as wings, legs, eyes, mouthparts, halters and genital ducts. When metamorphosis is complete, the adult fly emerges from pupal case (eclosion) (Figure 1). New female fly can start laying eggs 2 days after emerging while males are sexually active within hours of eclosion. After maturity, *D. melanogaster* is fertile during lifetime. Females reach the peak of egg production between the fourth and seventh day after their emergence. During this time, they lay eggs almost continuously at a rate of 50-70 eggs per day. Adult fruit fly may live for more than 10 weeks (Flagg, 1988; Tyler, 2000).

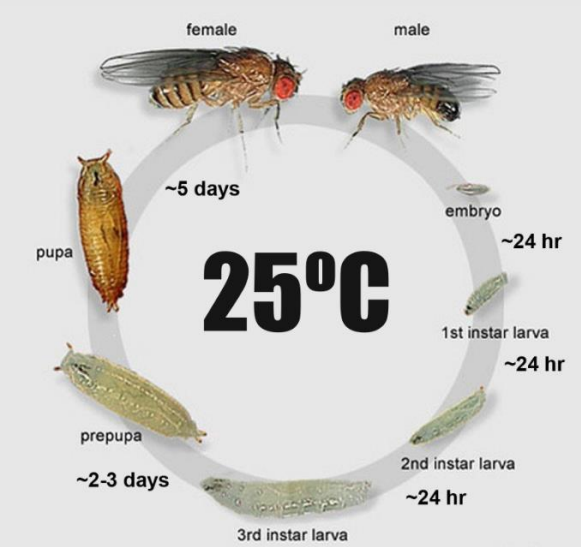

Figure 1. Life cycle of the *Drosophila melanogaster*. There are four distinct stages in the life cycle of *D. melanogaster*: embryo, three larva, pupa and *imago*. At 25ºC *D. melanogaster* will produce new adult in 9-10 days (modified, http://flymove.uni-muenster.de/).

1.3. General overview of wing disc

The adult wing of *D. melanogaster* is derived from the wing imaginal disc. This is the relatively flat epithelial sac that formed by two contiguous epithelia, a columnar layer, the disc proper (DP), and a squamous layer, the peripodial epithelium (PE) originated from embryonic cells. These embryonic cells are invaginated from embryonic epidermis and after cellular blastoderm stage, ectodermal cells are determined to become imaginal precursors. Wing disc primordium consists small cluster of cells, about 24 cells between 12 to 14 hours of embryogenesis and 40 cells in the first instar larva stage that proliferate during larval period up to 50 000 cells by the late larval stage when the disc is ready for differentiation (Bate and Arias, 1991; Neto-Silva, *et al*., 2009). After the beginning of pupariation, cell divisions cease and the differentiation of adult structures begins. Wing disc is separated into different regions which give rise to different adult structures: wing blade, wing margin, notum, scutellum, wing hinge and pleura. Due to this reason the wing disc is also called as a dorsal metathoracic disc. The wing blade and the wing margin are made from the wing pouch, which extends orthogonally to the plane of the disc. During this process, the mono-layered wing pouch folds along the dorsal-ventral compartment boundary to a two layered wing blade, while the other disc parts and other imaginal discs also form complex three-

dimensional structures. Finally, the former ventral part of the wing pouch forms the rear layer of the wing blade, which is closer to the pleura. Whereas the dorsal part of the wing pouch forms the front wing layer, which is closer to the notum. So the primordial dorsal and the primordial ventral cells end up connected at their basal side in the final wing (Tyler, 2000).

1.4. Wing disc compartmentalization

The imaginal disc of *Drosophila melanogaster* is divided into three different axes: anterior-posterior axis (A/P), dorsal-ventral axis (D/V) and proximal-distal axis (P/D). This compartmentalization is marked due to selector genes or also called as segment polarity genes. These are transcription factors that are active in specific compartments and usually at the same time to enable complex compartmentalization. The main drivers of wing disc compartmentalization are the Hedgehog (Hh), Notch, Epidermal Growth Factor Receptor (Egfr), Wingless (Wg) and Bone Morphogenetic Proteins (BMP) signals. Due to these signals the wing disk is divided at early stages into different compartments (Basler and Strul, 1994; Michel *et al*., 2016; Piddini and Vincent, 2009).

The first differentiation of cells in the wing disc takes place during embryogenesis which divides the wing disc into A/P compartment. This division is specified by a selector gene *engrailed* (*en*). *en* is expressed in the whole posterior compartment (Kornberg *et al*., 1985; Figure 2). *en* activity in posterior cell induce the expression of *hedgehog* (*hh*) which is expressed also in posterior cells. Hh is secreted over the border to the anterior side where it activates *decapentaplegic* (*dpp*) in absence of *en*. Dpp is a long-range morphogen that influence cell fate, growth and patterning in both compartments. (Basler and Strul, 1994; Zecca *et al*., 1995; Figure 2)

At the second instar larva developmental stage selector gene *apterous* (*ap*) starts to be expressed in the future dorsal part of the wing disc (Blair *et al*., 1994). Expression of *ap* depends on EGFR signaling during early wing disc development (Zecca and Struhl, 2002). The expression of *ap* induces the expression of Serrate (Ser), which is the ligand of Notch, in dorsal cells (Bachmann and Knust, 1998; Figure 2). Ser induces expression of Wg and Delta (Dl) close to ventral cells (Piddini and Vincent, 2009). Wg is a morphogen, expressed in a stripe of the border of D/V boundary cells and is necessary for the growth and patterning of the wing along the D/V axis. Dl which is also Notch ligand required in ventral cells induces Wg expression and maintain Ser in

dorsal cells. *ap* also induces Fringe expression in dorsal compartment. Fringe serves to polarize the activation of Notch by Dl and Ser at the D/V boundary (Michel *et al*., 2016). These early wing disc compartment boundaries define the wing blade primordium and initiate the following pattering of the wing vein (Dahmann and Basler, 1999; Wang *et al*., 2000).

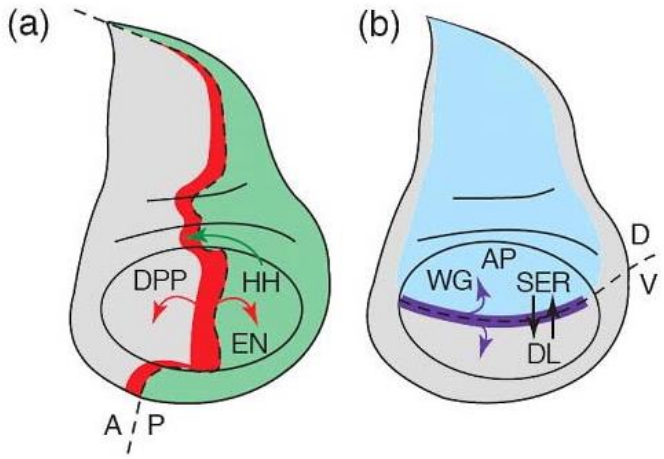

Figure 2. Compartmentalization of *Drosophila melanogaster* wing disc. (a) Anterior-posterior axis. Engrailed (En) is expressed in all posterior (P) cells and determines posterior identity. EN expression induces the expression of Hedgehog (Hh). Secreted Hh protein crosses the boundary and induces the expression of Decapetaplegic (Dpp) in anterior (A) cells along the anteroposterior boundary. Dpp acts as long-range organizing molecule, and controls growth and patterning of both compartments. (b) Dorsal-ventral axis. Apterous (Ap) is expressed in all dorsal area (D) cells and determines dorsal identity. Bidirectional signalling of Serrate (Ser) and Delta (Dl) leads to production of Wingless (Wg) at the dorsal-ventral boundary. Wg controls growth and patterning along the dorsal-ventral axis (modified by Dahmann and Basler, 1999).

1.5. Metamorphosis of wing

1.5.1. First apposition of the pupal wing

Once the larval brain gets a wing imaginal disc growth ending signal by the expression of *dilp8* the prothoracic gland cells are starting to emit steroid hormone called 20-hydroxyecdysone (20HE) that stimulates molting and metamorphosis (Colombani *et al.*, 2012; Dye *et al*., 2017; McBrayer *et al.*, 2007). At the beginning of metamorphosis, the wing imaginal disc starts to evert

and elongate which results in apposition of its dorsal and ventral compartments converting single-layered wing disc epithelium into a pupal bilayered proto-wing with two epithelial layers (Figure 3). This process is accomplished by a series of localized cell shape changes. This process takes place in first 4 hours of the prepupal period. At the end of the first apposition basal surfaces of dorsal and ventral epithelia stays in close proximity except for channel in the center. Epithelium cells are in columnar shape. (Aldaz *et al.,* 2010; Classen *et al.,* 2008; Fristom and Fristrom, 1992). Once the first apposition process is complete, the two apposed epithelia flatten and cell area increases (Figure 3). Cell shape change from columnar to cuboidal shape (Classen *et al.,* 2008). Developing wing expansions starting at the wing margins and extends inwards. Proveins are forming positions to adult longitudinal veins L3, L4 and L5. By the 4 hours of prepupal period, the 20HE titer falls and due to that pupal cuticle begins deposite at the apical cell surface. By the 7 hours the apical surface is convoluted and cuticulin layer surrounds the disc (Fristrom and Liebrich, 1986).

1.5.2. Inflation stage of the pupal wing

After first apposition, the inflation stage takes place. During this stage two layers of the wing separates and creates space (Figure 3). These two layers stay connected by cytoplasmic processes. Microtubules are formed at the apical hemidesmosomes which inserts into basal junctions forming transalar apparatus (Fristrom *et al.,* 1993). At 12 hours an influx of hemolymph forces the dorsal and ventral surfaces even more apart except in the regions that will give rise to veins (Etournay *et al., 2016*; Waddington, 1941). During inflation stage, the wing cells undergo many rounds of division (Milan *et al.,* 1996). It is known that Dpp promotes cell proliferation during inflation, but other regulators in addition to Dpp remain uncharacterized (Gui *et al*., 2019). The final mitoses occur between 15 and 14 hour with the peak at 17-18 hours (Gui *et al*., 2019; Schubiger and Palka, 1987). At 18 hours the 20HE titer rises again and pupal cuticle apolysis will continue which is the mark of reapposition stage (Bainbridge and Bownes, 1988).

1.5.3. Second apposition or reapposition of the pupal wing

At about 18-20 hours of AP the dorsal and ventral layers begin to reappose (Gui *et al*., 2019; Figure 3). During this process proliferation rate decreases and the pupal wing cells enter a

terminal differentiation stage into vein and intervein cells. Vein cells have a narrower apical cross-section and form corrugations that protrude from the dorsal and ventral surfaces of the wing blade (Etouranay *et al*., 2016). Cytoplasmic processes of intervene cells from the basal surfaces extends through the matrix until dorsal and ventral layers recontact again (Waddington, 1941). Wing veins are emerging and they remained as "opened spaces". By the end of this period intervein regions have reapposed (Fristrom, 1993). Until 40 hours AP extracellular space continues to diminish and only "opened spaces" are formed by veins (Waddington, 1993). Basal junctions are going to form between dorsal and ventral intervein cells and wing hairs or trichomes are going to form synchronously from the apical surface 30 000 cells over a period of about 20 hours (Mitchell *et al*., 1990; Mitchell *et al*., 1983). During the latter part of this period the cuticulin layer of the adult cuticle is deposited. Posterior crossvein cells are specified and start to differentiate after second apposition. Thereafter wing are going to expand laterally, increasing 2-3 fold in surface and become folded. Dorsal and ventral intervein cells separate basolaterally and creates space for extracellular matrix secreted by themselves (Bainbridge and Bownes, 1981). The remaining apicolateral cells are connected between adherents and septate junctions (Fristrom, 1993).

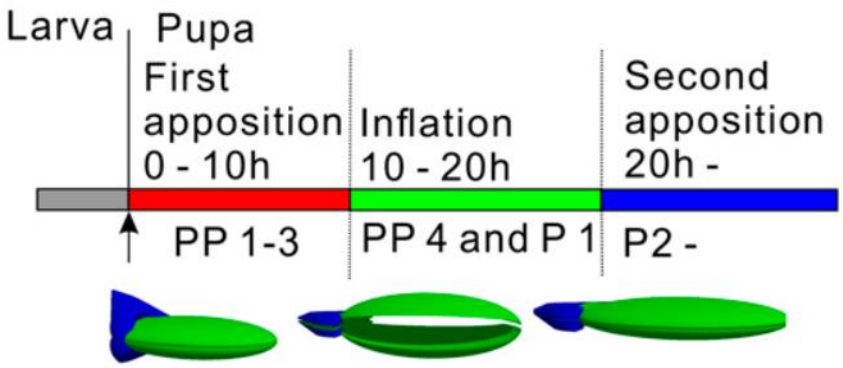

Figure 3. Metamorphosis of wing. At the beginning of metamorphosis, the wing imaginal disc starts to evert and elongate which results in apposition of its dorsal and ventral compartments converting single-layered wing disc epithelium into a pupal bilayered proto-wing with two epithelial layers. After first apposition, the inflation stage takes place. During this stage two layers of the wing separates and creates space. At about 18-20 hours of AP the dorsal and ventral layers begin to reappose (modified by Gui et al., 2019).

1.6. Integrins

Integrins are family of transmembrane cell adhesion receptors that mediate endothelial cells (EC) adhesion to extracellular matrix (ECM) proteins. Integrins are essential for many cellular functions. Integrin-based adhesions acts like anchor points for assembling and organizing the cytoskeleton, cell shape and migration. Additionally integrins control function and fate of cells by controlling and influencing their proliferation, apoptosis and differentiation. Integrin is like a bidirectional allosteric signaling machine that transmits signals inside-out and outside-in of cells. They have the ability to translate the attachment of external ligands to internal information which induces vital cellular mechanisms. They interact with the ECM through their extracellular domains and with components of the cell cytoskeleton and signaling molecules through their intracellular domains (Johnson and Lewis, 2002; Streuli, 2009).

Integrins are heterodimers which means that they have two non-covalently bonded subunits: alpha (α) and beta (β) (Cheresh and Mecham, 1994; Hynes, 1992). Integrins may differ in their specifity for ECM ligands. For instance, mammals have been found eighteen α and eight β subunits, while nematodes have two α and one β subunit and *D. melanogaster* has five α and two β subunits. These subunits are type I transmembrane glycoproteins that has larger extracellular domain and shorter cytoplasmic domain and a transmembranous domain (Narashima *et al*., 2013).

1.6.1. Myospheroid and its function in *Drosophila melanogaster*

Myospheroid (Mys) protein also called as βPS integrin or beta-integrin is 846 amino acid long protein situated on X-chromosome between nucleotides 8061645 and 8070237 (Uniprot.org). *mys* locus encodes a beta (β) subunit of the integrin dimer and with high probability forms heterodimers with all 5 known α subunits. Three of these heterodimers have been purified biochemically: PS1 (αPS1βPS), PS2 (αPS2βPS), and PS3 (αPS3βPS). (Broweret *et al*., 1984; Starket *et al*., 1997; Wilcoxet *et al*., 1984). With the absence of βPS integrin there are many developmental defects in *Drosophila melanogaster*: delay of primordial midgut migration, detach from the midgut endoderm of visceral muscles, defective dorsal closure, gut defects occur and

additionally adhesion between the two layers of wing fails when integrin function is reduced. (Brown *et al*., 2000; Martin-Bermudo *et al*., 1999).

2. Experimental part

2.1. Aims of the thesis

The aim of this thesis is describe the effect of βPS integrin *myospheroid* to epithelial morphogenesis in wing development of *Drosophila melanogaster* using thermosensitive wing specific gene knockdown phenotypes:

$$♀\ \frac{\text{ubi>}\propto\text{Tubulin:GFP}}{+};\frac{nubbin\text{−Gal4}}{\text{UAS}-mys\ \text{RNAi}};\frac{\text{gal80}^{\text{ts}}}{+}$$

and

$$♂\ \frac{\text{ubi>}\propto\text{Tubulin}}{y};\frac{nubbin\text{−Gal4}}{\text{UAS}-mys\ \text{RNAi}};\frac{\text{gal80}^{\text{ts}}}{y}$$

The more specific aims were following:

1. To screen 23 different fly strains Rab and Rho subfamily members and integrin specific mutant with a purpose to find interesting protein affecting the size of adult wing of *Drosophila melanogaster*.
2. To determine whether *mys* integrin knockdown causes abnormalities in the population of intervene cells of *Drosophila melanogaster*.
3. To describe spatiotemporal effect on size of adult wing blade, pupal wing pouch area and pupal wing of *mys* integrin in *mys* RNAi *Drosophila melanogaster*.

2.2. Materials and methods

2.2.1. Crossing flies

In this thesis Gal4/UAS system was used (Brand and Perrimon, 1993), combined with the thermosensitive version of Gal80 ($Gal80^{ts}$), (McGuire *et al*., 2004), a repressor of Gal4 protein activity, to precisely control, in time and space, the expression of UAS-*geneX*.

10 virgin female adult flies ubi>αTubulin:GFP/+; *nubbin*-Gal4; $Gal80^{ts}$/+ were crossed with 15 UAS-*geneX* construct carrying male flies. After setting a cross to mash-yeast-agar medium containing vial adult flies were allowed to lay eggs at 22°C over a period of 24 hours then flies were transferred into a new vial. Control flies (yellow white mutant) flies not carrying the UAS-*mys* RNAi transgene were also allowed to lay eggs in parallel. The offspring of both the experimental and control conditions was raised at 22°C to maintain the Gal4/UAS system switched off and then transferred to 29°C for different periods (24h, 16h, 8h before puparium formation) during larval development to activate Gal4/UAS-dependent gene expression.

2.2.2. Fly Strains

For integrin RNAi screening the flies were obtained from Vienna Drosophila RNAi Center (VDRC). Used integrin UAS responding lines were following: (#103704) UAS-*mys* RNAi, (#109608) UAS-*mew* RNAi, (#100770) UAS-*if* RNAi, (#100949) UAS-*scab* RNAi.

For Rab, Ras and Rho subfamily protein screening the flies were obtained from Bloomington Stock Center. Used UAS responding lines were following: (#4845) UAS-*cdc42* CA (constitutively active), (#6288) UAS-*cdc42* DN (dominant negative), (#9773) UAS-*rab5* CA, (#9771) UAS-*rab5* DN, (#51847) UAS-*rab5* RNAi, (#27051) UAS-*rab7* RNAi, (#9781) UAS-*rab8* CA, (#23271) UAS-*rab8* DN, (#23273) UAS-*rab9* CA, (#23643) UAS-*rab9* DN, (#42942) UAS-*rab9* RNAi, (#9790) UAS-*rab11* WT (wild type), (#9891) UAS-*rab11* CA, (#23261) UAS-*rab11* DN, (#27730) UAS-*rab11* DN, (#6291) UAS-*rac1* CA, (#6292) UAS-*rac1* DN, (#34910) UAS-*rac1* RNAi, (#32324) UAS-*rok* RNAi.

Fly strains (male individuals) named above were crossed with virgin female ubi>αTubulin:GFP/+; *nubbin*-Gal4; $Gal80^{ts}$/+ made in Osamu Shimmi's laboratory.

Gal4 drivers (#25754) nub-GAL4 and temperature-sensitive GAL80 repressor (#7017) tubP-GAL80ts were obtained from Bloomington Stock Center.

2.2.3. Adult wing dissection

Adult flies were collected from vials at the age of 120h after puparium formation (APF) and stored in absolute ethanol. For wing dissection the absolute ethanol was replaced with 70% ethanol about 1–3 day before dissection process. 70% ethanol removed and flies were washed 3 times using 1×PBS. Flies transferred to a pool of 1×PBS on a silicone based dissection plate. Using #5 forceps wings were dissected from hinge part and put to new 1×PBS pool. For examination, dissected wings were mounted in a 70% glycerol.

2.2.4. Larvae wing imaginal disc dissection

Collected 3rd instar larvae were placed in Petri dish filled with 1×PBS (dissection buffer) and allowed them to swim around for a few minutes for self-cleaning. Larvae transferred to a pool of 1×PBS on a silicone based dissection plate. Larva was clasped with #5 forceps. One pair of forceps was used to grab the mouth hooks while other pair of forceps was holding the animal still. Cuticle near the mouth hooks held steady while 2/3 of rest of the body quickly removed with forceps. Then overlying cuticle removed starting from head part and wing discs popped out. Thereupon biological material collected to a new tube and fixed using 3,7% formaldehyde (Sigma-Aldrich) in 1×PBT at 4ºC for overnight. Next day biological material washed with 1×PBT for 3×15 minutes. Then biological material transferred to a pool of 1×PBS on a silicone based dissection plate. Wing discs dissected from body and put them to 1×PBT tube. For examination, imaginal wing discs were mounted in an Antifade Mounting Medium (Vectashield).

2.2.5. Pupal wing dissection

Hardened cuticle was removed around the head part only and a hole was made into the back of the head using #5 forceps. Pupae were fixed for 2 days at 4°C in 3,7 % formaldehyde (Sigma-Aldrich) in 1×PBT. Pupae were washed with 1×PBT for 3×15 minutes at RT. Dissection of the wing was accomplished by removing the pupal case, making a hole into transparent cuticle near the wing hinge, grasping the wing hinge with forceps and gently pulling off the wing. The wings were stored in 1×PBT at 4ºC.

2.2.6. Sample imaging and microscopy

Microscope Nikon Eclipse 90i equipped with cameras Nikon Digital Sight D3-U3/DS-Fi2 and Hamamatsu Digital Camera C1140/ORCA-Flash4.OLT was used to observe and capture adult wing samples. Fluorescent images were obtained with a Leica SP8 upright laser confocal microscope. All images were processed and analyzed with ImageJ (NIH) software and plugin Fiji Wings version 2.3 was used to analyze trichome density in intervein areas of adult wing.

2.2.7. Pilot screening

10 female adult flies ubi>αTubulin:GFP/+; *nubbin*-Gal4; Gal80^{ts}/+ carrying a *nubbin*-Gal4 driver and the tub-Gal80^{ts} construct were crossed with 15 UAS-*geneX* construct carrying male flies. After setting a cross to mash-yeast-agar medium containing vial adult flies were allowed to lay eggs at 22°C over a period of 24 hours then flies were transferred into a new vial. Control flies not carrying the UAS-*mys* RNAi transgene were also allowed to lay eggs in parallel. The offspring of both the experimental and control conditions was raised at 22°C to maintain the Gal4/UAS system switched off and then transferred to 29°C for 16h-24h to activate Gal4/UAS-dependent gene expression. After being at 29ºC for 16h-24h, white prepupae were picked up and put back to 29ºC chamber. Flies kept there 100h and thereupon adult wing samples were made, using one wing from each female (n=10) and male (n=10) flies. Thereafter size and phenotype was assessed.

2.2.8. Determination of larva wing imaginal disc pouch area size

For measuring larva imaginal wing disc the flies with genotypes ubi>αTubulin:GFP/+; *nubbin*-Gal4/UAS-*mys* RNAi; $Gal80^{ts}$/+ and ubi>αTubulin:GFP/+; *nubbin*-Gal4/UAS-mys RNAi; $Gal80^{ts}$/+ were transferred from 22ºC to 29ºC chamber 0h, 8h, 16h and 24h BPF. Afterwards imaginal wing discs were dissected, fixed and mounted.

Under the confocal microscope using GFP fluorescence wing pouch, hinge and notum area were detected. As the wing blade develops from pouch area, an outline was drawn around the border of wing pouch area using polygon selection tool (Figure 4). The results obtained in square pixels (px^2). However, the resolution of image was already known in µm in addition to px. To convert px^2 to square micrometers ($µm^2$), the number of px divided by the number of µm and the answer got squared. The squared answer multiplied with the wing pouch size in px^2.

Figure 4. Measuring wing imaginal disc pouch area. As the wing blade develops from pouch area, an outline was drawn around the border of wing pouch area for measuring the wing imaginal disc pouch area (red circle), using ImageJ polygon selection tool. (Scale bar 100 $µm^2$).

2.2.9. Determination of pupal wing size

For measuring larva imaginal wing disc the flies with genotypes ubi>αTubulin:GFP/+; *nubbin*-Gal4/UAS-*mys* RNAi; $Gal80^{ts}$/+ and ubi>αTubulin:GFP/+; *nubbin*-Gal4/UAS-mys RNAi; $Gal80^{ts}$/+ and YW were transferred from 22ºC to 29ºC chamber 0h, 8h, 16h and 24h BPF. Afterwards 24h pupal wings (21h at 29ºC) were dissected, fixed and mounted.

Under the confocal microscope using GFP fluorescence developing wing blade and hinge part were detectable. For measuring pupal wing blade, an outline was drawn around the border of wing blade using polygon selection tool. The results obtained in px^2. However, the resolution of image was already known in µm in addition to pixels. To convert px^2 to $µm^2$, the number of px divided by the number of µm and the answer got squared. The squared answer multiplied with the pupal wing blade size in px^2.

2.2.10. Determination of adult wing size

Under the microscope, wing blade and hinge areas were detected. For measuring adult wing size, an outline was drawn around the border of wing blade using polygon selection tool. The results obtained in px^2. However, the resolution of image was already known in µm in addition to pixels. To convert px^2 to $µm^2$, the number of px divided by the number of µm and the answer got squared. The squared answer multiplied with the pupal wing blade size in px^2.

2.2.11. Identification of trichome density and cell size within intervein regions

The intervein areas in wing blade categorized as follows: marginal, submarginal, first posterior, second posterior, first basal and costal area. Third posterior and axillary region considered as one area just like second basal and discal area, because their borderlines were not clearly detectable (Figure 5).

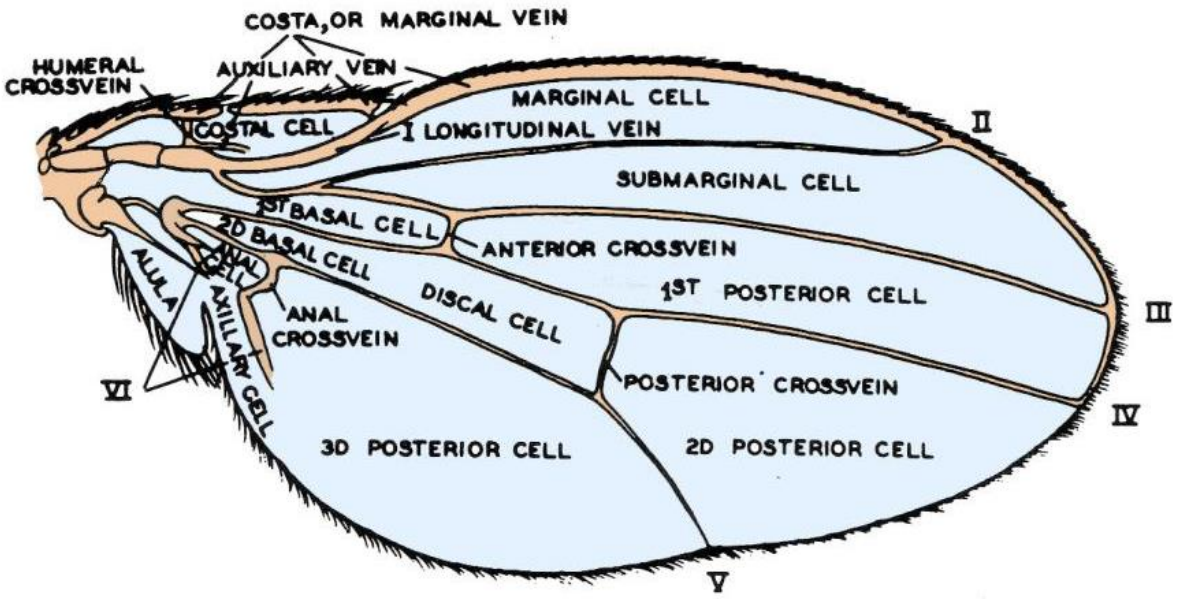

Figure 5. Intervein areas in Drosophila melanogaster wing. The intervein areas in wing blade categorized as follows: marginal, submarginal, first posterior, second posterior, third posterior area, axillary area, first basal, second basal, discal and costal area (Bridges, 2013).

Intervein areas described above were measured by drawing borderline to the border of intervein area and vein contact surface using polygon selection tool. The results obtained in px^2. However, the resolution of image was already known in µm in addition to pixels. To convert px^2 to $µm^2$, the number of px divided by the number of µm and the answer got squared. The squared answer multiplied with the pupal wing blade size in px^2.

For calculating trichome density, borderline to the border of intervein area were drawn and using order "polygon trichome density." It gave the amount of trichomes per intervein are which was divided by result of intervein area.

For calculating average intervene cell size, the amount of trichomes were divided by the size of intervein area in $µm^2$.

2.2.12. Statistical analysis

Data distribution was calculated using Shapiro-Wilk test with the help of GraphPad Prism version 8.4.3 for Windows. Standard deviations (SD) were calculated and Student's t-test or Mann-Whitney U test were calculated with the help of GraphPad Prism. Statistical significance was

carried out if p-value was equal or less than 0,05 (*$p \leq 0.05$; **$p \leq 0.01$; ***$p \leq 0.001$). Graphical representations of data were done by using GraphPad Prism version 8.4.3 or Microsoft Excel 2013.

2.3. Results

2.3.1. Pilot screening

Rab and Rho subfamily proteins are transmembrane proteins member of Ras superfamily which regulates organelle development, cytoskeletal dynamics, cell movement and many other cellular function just like integrins. All of these three proteins have ability to affect proliferation (Haga and Ridley, 2016; Schwarts *et al*., 2007). It is known that *Drosophila* wing development includes active proliferation controlled by Dpp signaling. Dpp is indispensable for proper growth of the pupal wing (Gui *et al.*, 2019). The aim of the screening was to find suitable protein which affect pupal wing size and have possible co-signalling mechanism with Dpp.

In primary screening 13 Rab (*rab11* WT; *rab11* CA; *rab11* DN; *rab11* RNAi; *rab5* CA; *rab5* DN; *rab5* RNAi; *rab7* RNAi; *rab8* CA; *rab8* DN; *rab9* CA; *rab9* DN; *rab9* RNAi), 6 Rho (*rac1* DN; *rac1* CA; *rac1* RNAi; *rok* RNAi; *cdc42* CA; *cdc42* DN) subfamily and 4 different integrin (*mys* RNAi; *mew* RNAi; *if* RNAi; *scab* RNAi) specific mutant fly strains (males n=15) carrying UAS-*geneX* construct were crossed with ubi>αTubulin:GFP; *nubbin*-Gal4; Gal80^{ts} female (n=10) driver flies. As a consequence of general screening, the flies had various wing phenotypes. Some wings were blistered (UAS-*rok1* RNAi; UAS-*rac1* DN). Some flies had wing vein formation (UAS-*rab9* RNAi; UAS-*rab9* DN; UAS-rab8 DN; UAS-*rab9* RNAi; UAS-*cdc42* DN) defects. 4 genotypes died at embryonic age (UAS-*rab11* WT; UAS-*rab11* DN; UAS-*rab11* RNAi; UAS-*rac1* CA) and wing blades of UAS-*mew* RNAi and UAS-*if* RNAi were not measurable due to heavy deformations. Only a 3 fly wings were increased (UAS-*rab8* CA; UAS-*rac1* RNAi; UAS-*scab* RNAi) and 3 reduced in size (UAS-*cdc42* DN; UAS-*rab9* RNAi; UAS-*mys* RNAi) comparing to control (Figure 6).

The average wing blade size of control flies were 1,4894 mm^2 (±0,0923) in females (n=10) and 1,231mm^2 (±1,2031) in males (n=10). Comparing with control group statistical significance with following flies carrying UAS-*geneX* construct: UAS-*cdc42* DN males 1,0506 mm^2 (±0,0736) (p=0,00094), UAS-*rab5* RNAi females 1,5918 mm^2 (±0,0287) (p=0,0292), UAS-*rab8* CA females 1,626 mm^2 (±0,068) (p=0,0066) and males 1,3265 mm^2 (±0,0608) (p=0,0003), UAS-*rab9* RNAi females 1,4 mm^2 (±0,074) (p=0,045), UAS-*rac1* RNAi females 1,642 mm^2 (±0,065) (p=0,0036) and males 1,2691 mm^2 (±0,0545) (p=0,0221), UAS-*mys* RNAi females 1,2034 mm^2

(±0,2347) (p=0,0067) and males 0,8906 mm^2 (±0,1207) ($p=2,04\times10^{-5}$), UAS-*scab* RNAi females 1,6078 mm^2 (±0,1102) (p=0,015).

According to the result of measures UAS-*rab5* RNAi females, UAS-*rab8* CA females and males, UAS-*rac1* RNAi females and males were had increased wing blade and UAS-*cdc42* DN males, UAS-*rab9* RNAi females and both females and males UAS-*mys* RNAi flies showed decreased wing blade size.

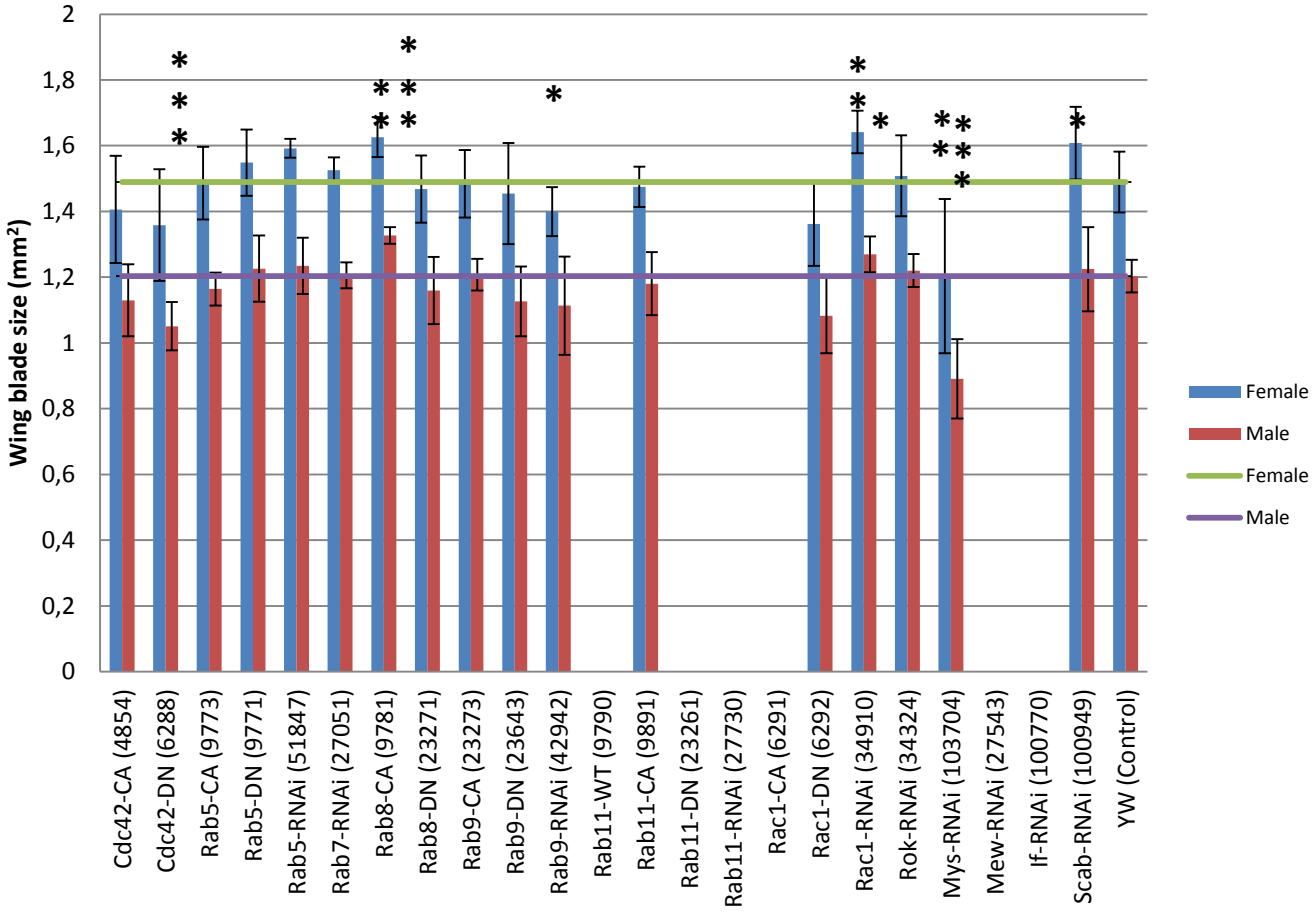

<u>Figure 6.</u> Pilot screening of mutant flies. 13 Rab, 6 Rho subfamily and 4 different integrin specific mutant fly strains (male (n=15) carring UAS-*geneX* contruct were crossed with ubi>αTubulin:GFP; *nubbin*-Gal4; $Gal80^{ts}$ female (n=10) driver flies and adult flies wing size were measured(15 female and 15 male wings were used per each genotype). According to the data UAS-*rab5* RNAi females, UAS-*rab8* CA females and males, UAS-*rac1* RNAi females and males were had increased wing blade and UAS-*cdc42* DN males, UAS-*rab9* RNAi females and both females and males UAS-*mys* RNAi flies showed decreased wing blade size. The size of the control wing are 1,4894

mm^2 (±0,0923) in females and 1,231$mm^{2.}$ Mõõtmatud või surnud. (±1,2031) in males. (*p≤0.05; **p≤0.01; ***p≤0.001).

According to the pilot screening of mutant flies, 6 female genotypes with statistically significant size of the wing blade were mentioned: ubi>αTubulin:GFP; *nubbin*-Gal4/UAS-rab5 RNAi; tub-80^{ts}/+ ; ubi>αTubulin:GFP; *nubbin*-Gal4/UAS-*rab8* CA; tub-80^{ts}/+ ; ubi>αTubulin:GFP; *nubbin*-Gal4/UAS-*rab9* RNAi; tub-80^{ts}/+ ; ubi>αTubulin:GFP; *nubbin*-Gal4/UAS-*rac1* RNAi; tub-80^{ts}/+ ; ubi>αTubulin:GFP; *nubbin*-Gal4/UAS-*mys* RNAi; tub-80^{ts}/+ ; ubi>αTubulin:GFP; *nubbin*-Gal4/UAS-*scab* RNAi; tub-80^{ts}/+. Looking the phenotype of statistically significant female adult flies, one can detect that visually the most different phenotype has ubi>αTubulin:GFP; *nubbin*-Gal4/UAS-*mys* RNAi;tub-Gal80^{ts}/+ . One can be see that trichome orientation and positioning of *mys* RNAi phenotype are defect (black arrow at Figure 7.F). Additionally, this genomes' adult wing was only smaller than control (Figure 7).

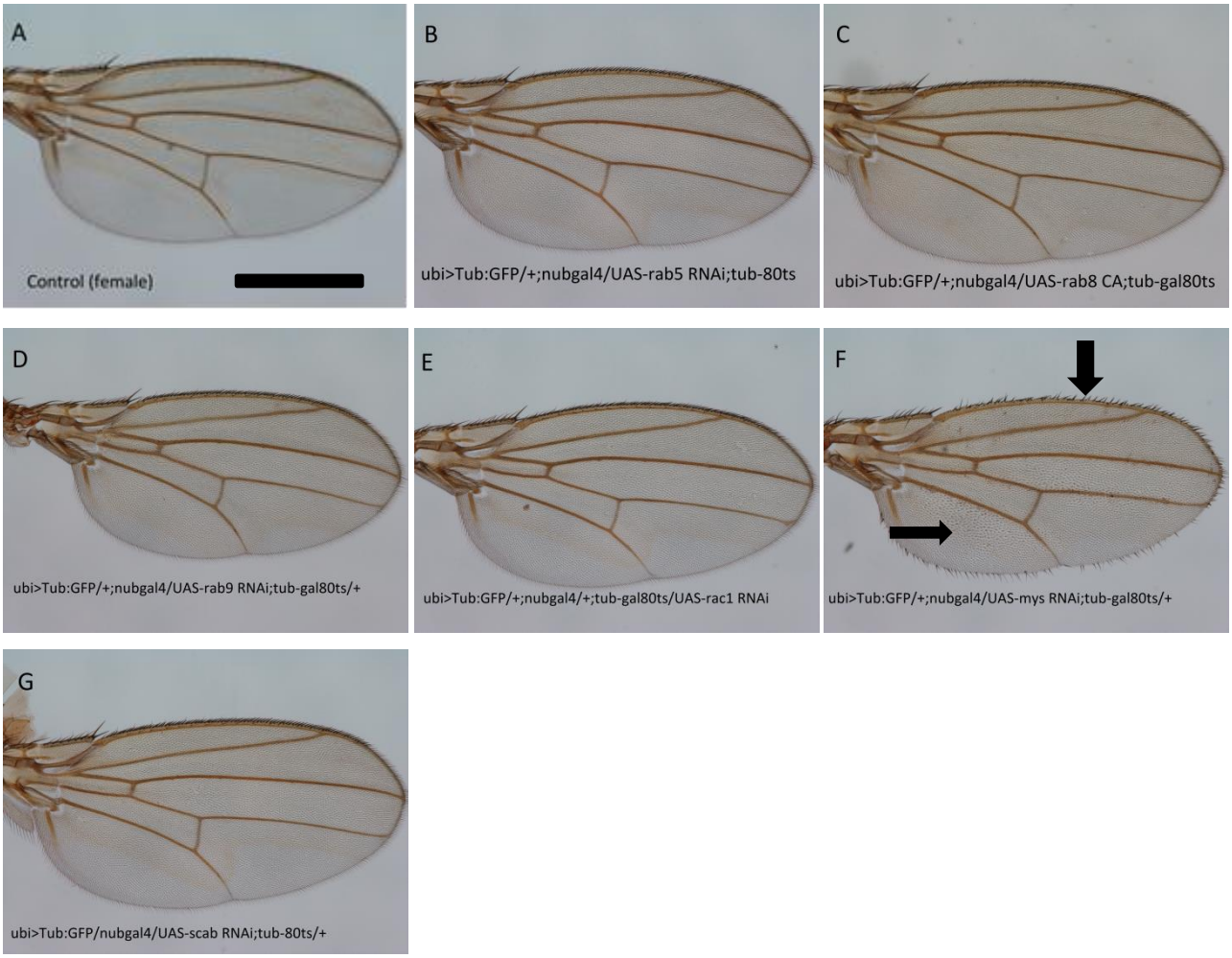

Figure 7. Phenotype of statistically significant female adult wings. According to the pilot screening, the 6 different genotypes in size comparing to control fly were carried out: (B) ubi>αTubulin:GFP; *nubbin*-Gal4/UAS-*rab5* RNAi; tub-80^{ts}/+ ; (C) ubi>αTubulin:GFP; *nubbin*-Gal4/UAS-*rab8* CA; tub-80^{ts}/+ ; (D) ubi>αTubulin:GFP; *nubbin*-Gal4/UAS-*rab9* RNAi; tub-80^{ts}/+ ; (E) ubi>αTubulin:GFP; *nubbin*-Gal4/UAS-*rac1* RNAi; tub-80^{ts}/+ ; (F) ubi>αTubulin:GFP; *nubbin*-Gal4/UAS-*mys* RNAi; tub-80^{ts}/+ ; (G) ubi>αTubulin:GFP; *nubbin*-Gal4/UAS-*scab* RNAi; tub-80^{ts}/+. (Scale bar 500 μm).

According to the pilot screening of mutant flies, 4 male genotypes with statistically significant size of the wing blade comparing to adult wing size were mentioned: ubi>Tubulin:GFP/y; *nubbin*-Gal4/UAS-*rab8* CA; tub-gal80^{ts}/+ ; ubi>Tubulin:GFP/y; *nubbin*-Gal4/+; tub-gal80^{ts}/UAS-rac1 RNAi; ubi>Tubulin:GFP/y; *nubbin*-Gal4/UAS-*cdc42* DN; tub-gal80^{ts}/+ ; ubi>Tubulin:GFP/y; *nubbin*-Gal4/UAS-*mys* RNAi; tub-gal80^{ts}/+. Looking the wing phenotype of statistically significant male adult flies, one can detect that visually the most different genotypes are ubi>Tubulin:GFP/y; *nubbin*-Gal4/UAS-*cdc42* DN and ubi>Tubulin:GFP/y; *nubbin*-Gal4/UAS-*mys* RNAi; tub-gal80^{ts}/+. Both wings are smaller in size and they also trichome orientation defects are detectable (black arrows at Figure 8. D and E). ubi>Tub:GFP/y; nubbin-Gal4/UAS-*cdc42* DN individ has defects in marginal and submarginal area in addition posterior cross vein sharpening.

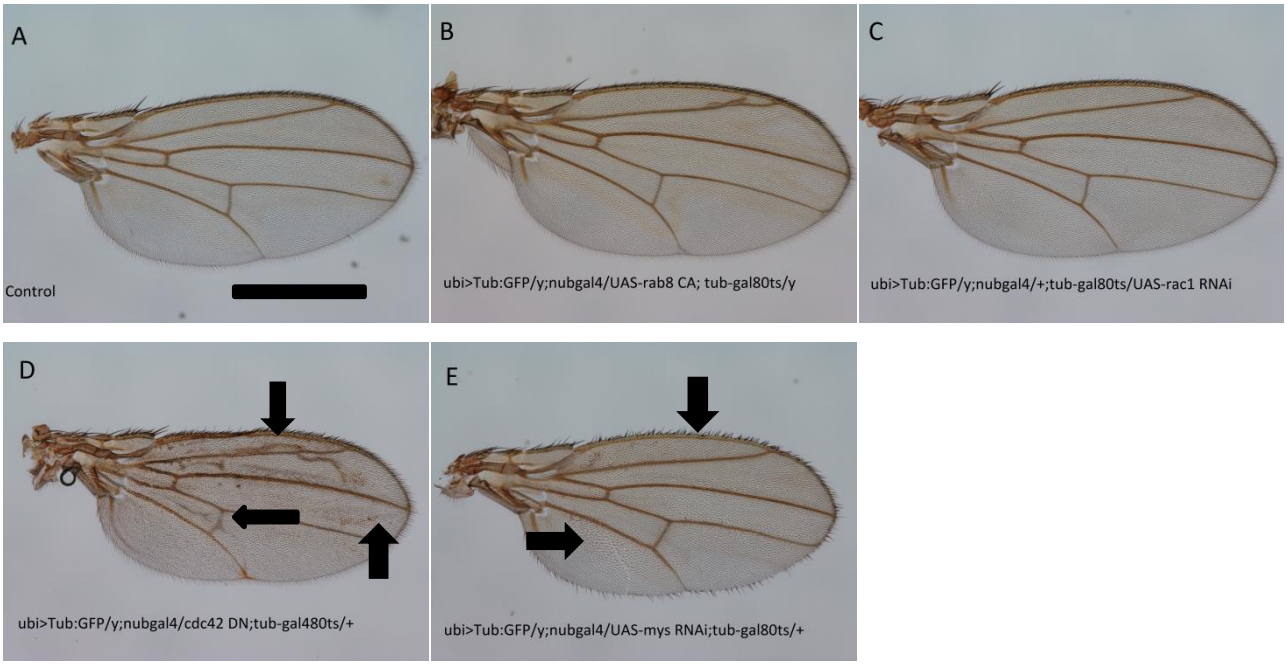

Figure 8. Phenotype of statistically significant male adult wings. According to the pilot sceening, the 4 different genotypes in size comparing to control fly were carried out: (B) ubi>Tub:GFP/y; nubbin-Gal4/UAS-rab8 CA; tub-gal80ts/+ ; (C) ubi>Tub:GFP/y; nubbin-Gal4/+; tub-gal80ts/UAS-rac1 RNAi; (D) ubi>Tub:GFP/y; nubbin-Gal4/UAS-cdc42 DN; tub-gal80ts/+ ; (E) ubi>Tub:GFP/y; nubbin-Gal4/UAS-mys RNAi; tub-gal80ts/+. (Scale bar 500 µm).

According to previous data it is decided to continue the experiments with ubi>Tub:GFP/+; nubbin-Gal4/UAS-mys RNAi; tub-gal80ts/+ and ubi>Tub:GFP/y; nubbin-Gal4/UAS-mys RNAi; tub-gal80ts/+ due to their small size and specific phenotype.

2.3.2. Spatiotemporal effect of *mys* integrin knockout to wing size of the *Drosophila melanogaster*

For detecting spatiotemporal effect of *mys* integrin knock-out to wing size of the *Drosophila melanogaster*, wing imaginal disc pouch area exactly before pupariation, 24h APF pupal wing area and adult wing blade area were measured using different timing of *mys* RNAi knockout. Previously named developmental stages were transferred from 22ºC environment to 29ºC environment 24h, 16h, 8h and 0h before pupariation to switch on *nubbin*-Gal4 driver and then samples were made. Also samples were made with fly wings no heating previously.

Firstly, female (n=15) and male (n=15) adult wing blades were measured using different time of BPF switching off *mys* expression in wing disc pouch area. Measured wing blades shows statistical difference of start putting flies at 0 hours or beginning of pupariation at 29ºC. At this time wing morphogenesis just starts and longer time BPF at 29ºC increased the statistical difference. Keeping flies at 22ºC, the same temperature at which flies were crossed, did not show statistical significance. That means crossing and keeping flies at 22ºC before transferring vials to 29ºC did not switch off the *mys* expression.

The results of female adult wing measures were following: average wing blade size at 22ºC control group 1,979 (±0,0551) mm^2 and *mys* RNAi 1,961 (±0,045) mm^2 (p=0,337). 0h BPF control group wing blade size were 1,728 (±0,057) mm^2 and mys RNAi 1,631 (±0,077) mm^2 (p=0,00056). Putting larvae at 29ºC 8h BPF results were control group 1,643 (±0,0501) mm^2 and *mys* RNAi 1,5607 (±0,0538) mm^2 (p=0,00018). 16h BPF control group 1,5581 (±0,067) mm^2 and *mys* RNAi 1,2203 (±0,074) mm^2 ($p=2\times10^{-12}$). 24h BFP control group 1,551 (±0,096) mm^2 and *mys* RNAi group 0,8481 (±0,092) mm^2 (p<0,0001) (Figure 9).

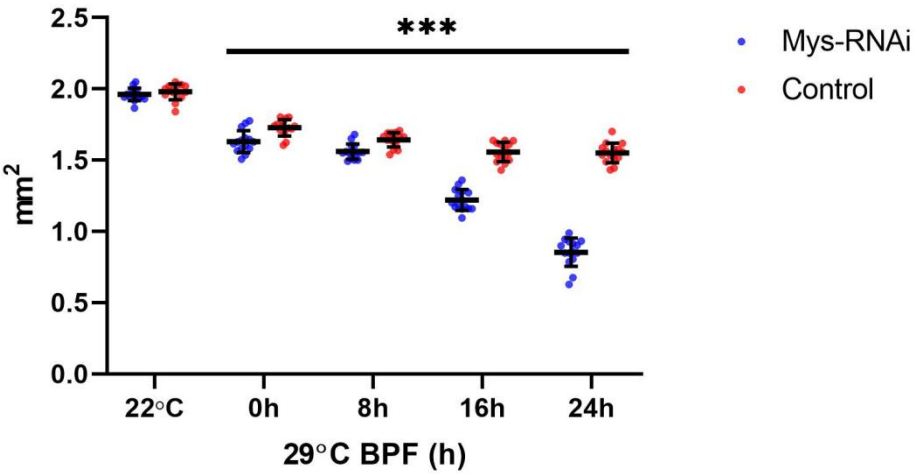

Figure 9. Female adult wing blade sizes at different *mys* knock-out timing. Female (n=15) adult wing blades with *mys* knock-out were measured 120h APF using different time of BPF switching off *mys* expression in wing disc pouch area. Measured wing blades shows statistical difference of start putting flies at 0 hours or white pupa formation at 29ºC. (*p≤0.05; **p≤0.01; ***p≤0.001)

The results of male adult wing measures were following: average wing blade size at 22ºC control group 1,579 (±0,054) mm^2 and *mys* RNAi 1,569 (±0,041) mm^2 (p=0,589). 0h BPF control group

wing blade size were 1,728 (±0,0573) mm^2 and mys RNAi 1,267 (±0,075) mm^2 (p=0,0035). Putting larvae at 29ºC 8h BPF results were control group 1,268 (±0,039) mm^2 and *mys* RNAi 1,182 (±0,059) mm^2 ($p=5,7\times10^{-5}$). 16h BPF control group 1,213 (±0,053) mm^2 and *mys* RNAi 0,99 (±0,111) mm^2 ($p=7,7\times10^{-7}$). 24h BFP control group 1,217 (±0,057) mm^2 and *mys* RNAi group 0,726 (±0,112) mm^2 ($p=9,9\times10^{-13}$) (Figure 10).

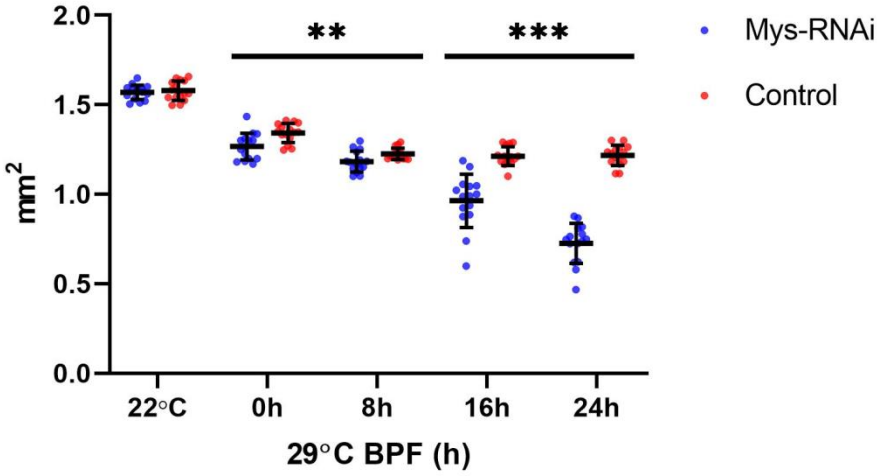

Figure 10. Male adult wing blade size at different *mys* knock-out timing. Male (n=15) adult wing blades with *mys* knock-out were measured 120h APF using different time of BPF switching off *mys* expression in wing disc pouch area. Measured wing blades showed statistical difference of start putting flies at 0 hours or white pupa formation at 29ºC. (*p≤0.05; **p≤0.01; ***p≤0.001)

For describing spatiotemporal effect on the wing development, pupal wings were measured as next step. At this experiment, pupae age that samples were made were 24h APF (21h at 29ºC) old. Larvae were kept at 29ºC for 0h, 8h, 16h or 24h before white pupa formation. Then white pupae were selected and put back to 29ºC environment for 21h.

As a result of describing pupal wing size at the age of 24h APF, statistical significance between control group and *mys* RNAi group were detected only in flies that got 24h 29ºC heating BPF.

The average results of the experiment with female flies were follow: average pupal wing blade size at 22ºC control group 285728 (±14847) μm^2 and *mys* RNAi 272194 (±16640) μm^2 (p=0,0675). 0h BPF control group pupal wing blade size were 233060 (±10208) μm^2 and mys

RNAi 243145 (±15885) µm^2 (p=0,0596). Putting larvae at 29ºC 8h BPF results were control group 233169 (±7991) µm^2 and *mys* RNAi 240179 (±11809) µm^2 (p=0,069). 16h BPF control group 232737 (±6274) µm^2 and *mys* RNAi 238974 (±11721) µm^2 (p=0,0832). 24h BFP control group 232450 (±9191) µm^2 and *mys* RNAi group 208517 (±11699) µm^2 (p=1,24×10^{-6}) (Figure 11).

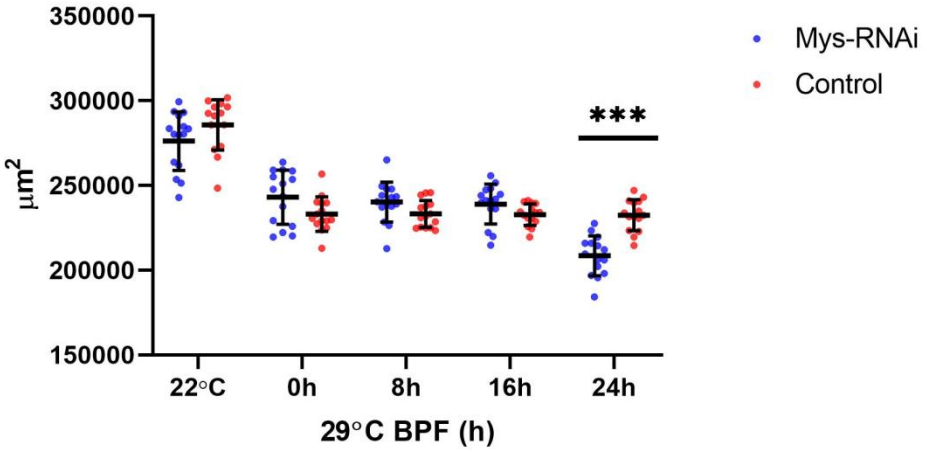

Figure 11. Female pupal wing size at different *mys* knock-out time. Female (n=15) pupal wing blades with *mys* knock-out and control group were measured 24h APF using different time of BPF switching off *mys* expression in wing disc pouch area. Measured pupal wing blades showed statistical difference preheating pupae 24h at 29ºC. (*p≤0.05; **p≤0.01; ***p≤0.001)

The average results of the experiment with male flies were follow: average pupal wing blade size at 22ºC control group 227211 (±7941) µm^2 and *mys* RNAi 229108 (±10288) µm^2 (p=0,577). 0h BPF control group pupal wing blade size were 198356 (±4921) µm^2 and *mys* RNAi 199856 (±5323) µm^2 (p=0,429). Putting larvae at 29ºC 8h BPF results were control group 196059 (±12022) µm^2 and *mys* RNAi 198673 (±13780) µm^2 (p=0,5125). 16h BPF control group 190826 (±9922) µm^2 and *mys* RNAi 188475 (±8697) µm^2 (p=0,4959). 24h BFP control group 190528 (±8985) µm^2 and *mys* RNAi group 172657 (±9846) µm^2 (p=1,67×10^{-5}) (Figure 12).

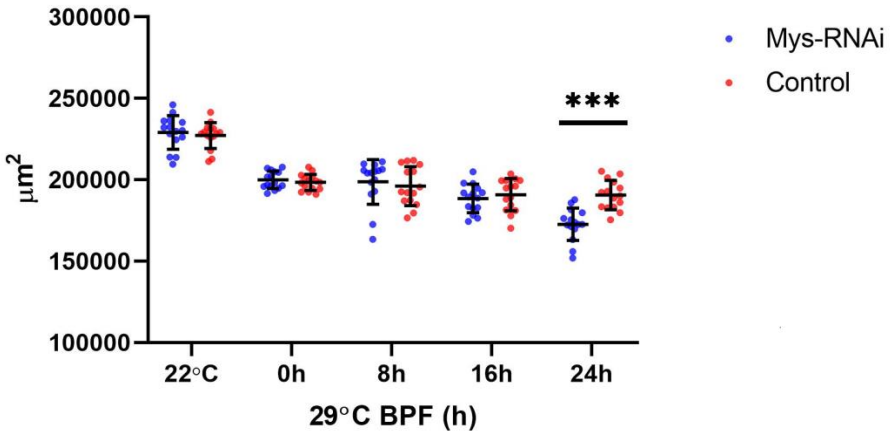

Figure 12. Male pupal wing size at different *mys* knock-out time. Female (n=15) pupal wing blades with *mys* knock-out and control group were measured 24h APF using different time of BPF switching off *mys* expression in wing disc pouch area. Measured pupal wing blades showed statistical difference preheating pupae 24h at 29ºC. (*p≤0.05; **p≤0.01; ***p≤0.001)

For next step 3rd instar larvae wing imaginal disc pouch area were measured exactly before pupariation process. At this experiment, wing imaginal discs were collected in larvae that who were kept at 29ºC for 0h, 8h, 16h or 24h before. As a result of describing wing imaginal disc pouch size at the age of 24h APF, statistical significance did not occur (Figure 13 and 14).

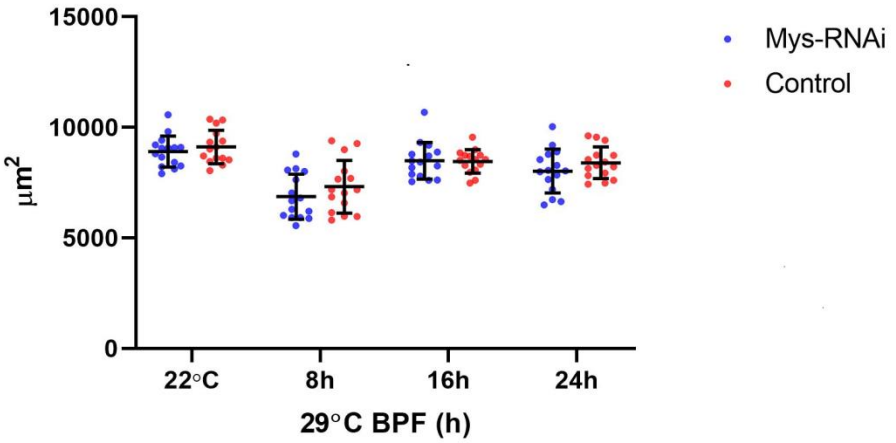

Figure 13. Female wing imaginal disc size at different *mys* knock-out time. For measuring 3rd instar larvae wing imaginal discs using different timepoints of switching off *mys* expression in wing pouch area, there were no statistical difference between control and *mys* RNAi group.

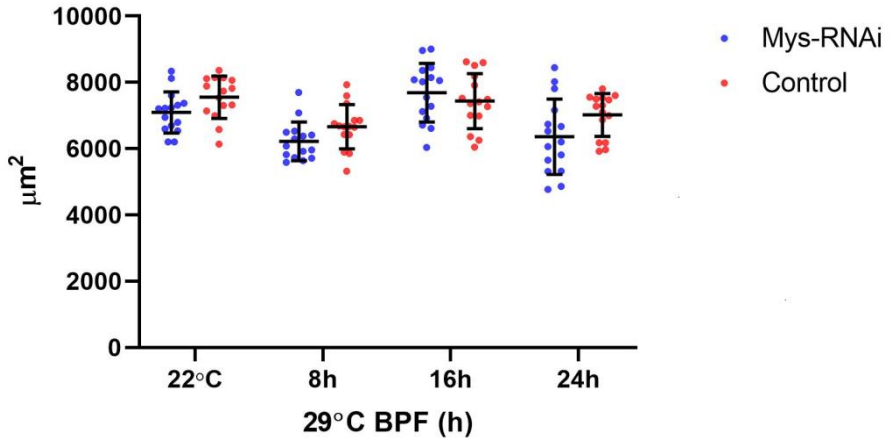

Figure 14. Male wing imaginal disc size at different *mys* knock-out time. For measuring 3rd instar larvae wing imaginal discs using different timepoints of switching off *mys* expression in wing pouch area, there were no statistical difference between control and *mys* RNAi group.

2.3.3. *mys* integrin knockdown causes abnormalities in the population of intervein cells

One way to evaluate the effect of mys to wing development is to find out whether disruption of mys expression causes any difference in intervein areas and their cell population. For describing this, genotype ubi>αTubulin:GFP/+; nubbin-Gal4/UAS-mys RNAi; tub-gal80ts/+ (female flies

n=15) preheated at 29ºC for 16h BPF, white pupae were collected and then put back at 29ºC. Adult wing samples were made and intervein areas were measured and trichome numbers counted each intervein area separately.

One area that showed statistical significance in size was submarginal area. In control flies area was 240107,92 (±12474) μm^2 and *mys* RNAi flies 200504,5 (±16829) μm^2 ($p=9{,}32\times10^{-8}$). The second areas that showed statistical significance in size was 1st posterior area. In control flies area was 255246,213 (±17388) μm^2 and *mys* RNAi flies 147106,9 (±22564) μm^2 ($p=3{,}37\times10^{-14}$). The third area that showed statistical significance in size was 2nd posterior area. In control flies area was 267422,976 (±14172) μm^2 and *mys* RNAi flies 188947 (±22386) μm^2 ($p=3{,}77\times10^{-11}$). The fourth area that showed statistical significance in size was 3rd posterior area. In control flies area was 328413 (±20745) μm^2 and *mys* RNAi flies 202311,315 (±35073). The next area that showed statistical significance in size was 1st basal area. In control flies area was 25767 (±1355) μm^2 and *mys* RNAi flies 27576 (±1981) μm^2 ($p=0{,}0074$). Checking the 2nd basal and distal area there was aslo statistical significance detectable. In control flies 93695 (±5718) μm^2 was the size of area and in *mys* RNAi flies 80847 (±6194) μm^2 ($p=2{,}44\times10^{-6}$) (Figure 15).

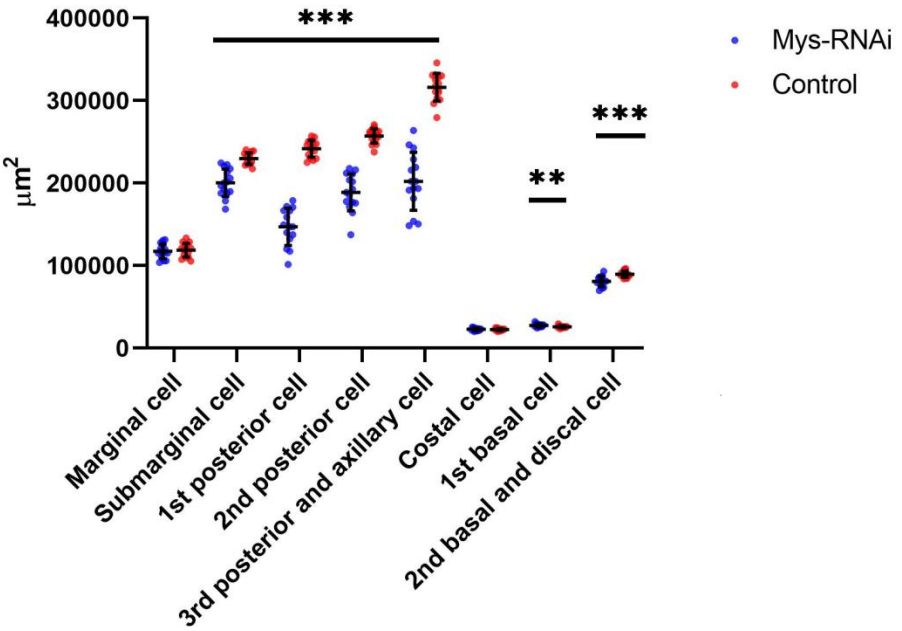

Figure 15. Adult wing intervein area size at 16h BPF *mys* knock-out time. One way to evaluate the effect of mys to wing development is to find out whether disruption of mys expression causes any difference in intervein areas. As a result, all intervein areas were statistically different except marginal and costal. (*p≤0.05; **p≤0.01; ***p≤0.001)

Assessing number of trichomes each intervein area separately, statistical significance were follow: submarginal area control group 2730 (±97) and *mys* RNAi group 2072 (±165) trchomes ($p=2{,}82\times10^{-12}$); 1st posterior area control group 2821 (±138) and *mys* RNAi group 1381 (226) trichomes ($p=1{,}36\times10^{-16}$); 2nd posterior area control group 3139 (±103) and *mys* RNAi group 1819 (±250) trichomes ($1{,}3\times10^{-11}$); 3rd posterior area control group 3960 (±110) and *mys* RNAi 2228 (±370) trichomes ($p=5{,}07\times10^{-12}$); 2nd basal and discal area control group 1123 and *mys* RNAi group 939 trichomes ($p=6{,}22\times10^{-8}$) (Figure 16).

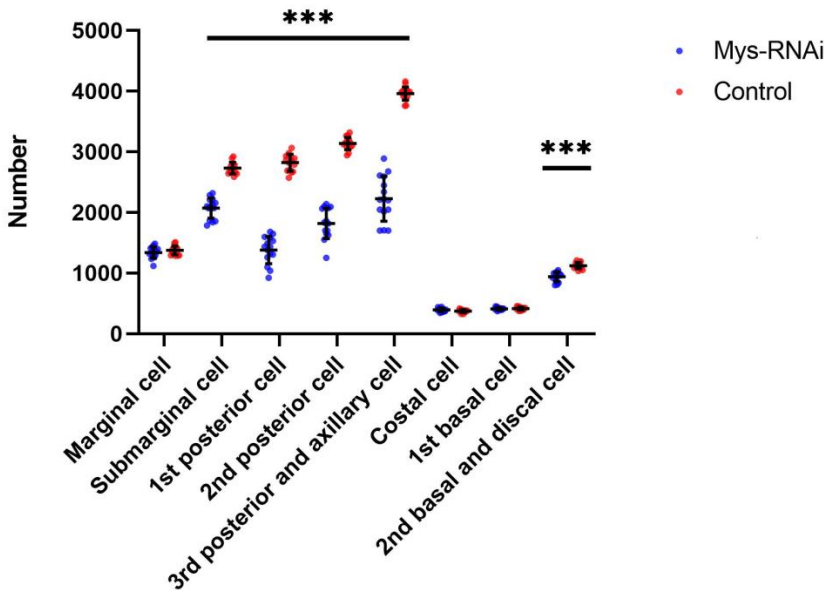

Figure 16. Intervein area trichome number at 16h BPF *mys* knock-out time. Evaluating the effect of *mys* to wing development is to find out whether disruption of mys expression causes any difference in number of intervein areas. As a result, all intervein areas were statistically different except marginal and costal. (*p≤0.05; **p≤0.01; ***p≤0.001)

As knowing the size of different intervein areas and the number of trichomes, thrichome density and cell size can be calculated.

The result of density of trichomes (trichome/µm^2) were significally different in every intervein area except marginal and 2nd basal and discal area. The results were follow: submarginal area control group 0,01139 (±6,1×10^{-4}) and *mys* RNAi group 0,01035 (±3,6×10^{-4}) (p=8,47×10^{-6}); 1st posterior area control group 0,01108 (±6,6×10^{-4}) and *mys* RNAi group 0,0094 (±2,9×10^{-4}) (p=2,77×10^{-8}); 2nd posterior area control group 0,01176 (±5,6×10^{-4}) and *mys* RNAi group 0,0096 (±2,9×10^{-4}) (p=5,95×10^{-12}); 3rd posterior area control group 0,0121 (±7,5×10^{-4}) and *mys* RNAi 0,01104 (±4,6×10^{-4}) (p=0,0001); 1st basal area control group 0,01611 (±5,02×10^{-}4) and *mys* RNAi group 0,015 (±5,01×10^{-4}) (p=2,97×10^{-6}). Also costal area showed statistical significance (p=0,045), but it is not part of the wing blade (Figure 17).

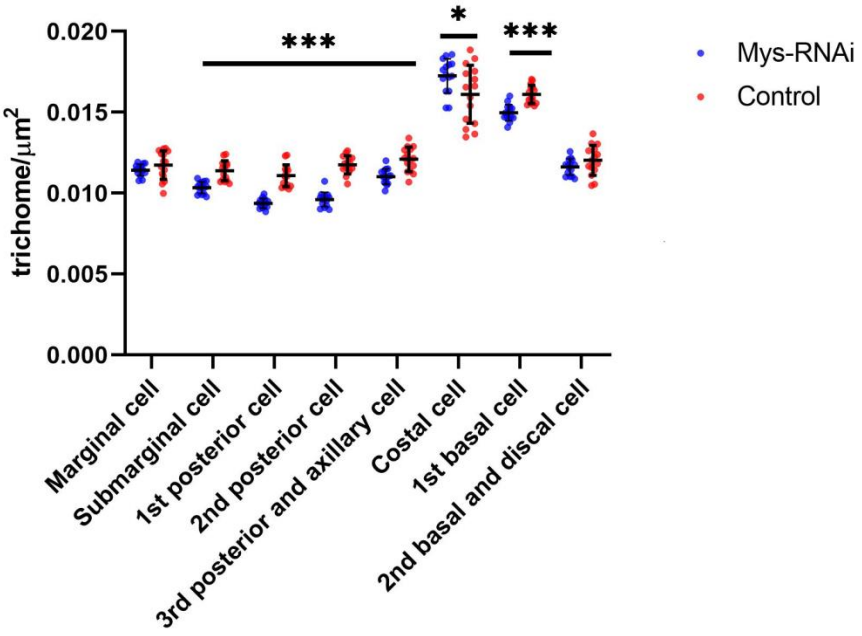

Figure 17. Intervein area trichome density at 16h BPF *mys* knock-out. Evaluating the effect of *mys* to wing development is to find out whether disruption of mys expression causes any difference inintervein trichome density. As a result, all intervein area trichome were statistically different except marginal and 2nd basal and discal area. (*p≤0.05; **p≤0.01; ***p≤0.001)

One area that showed statistical significance in cell size was submarginal area. In control flies cell size was 9,378 (±0,2501) µm^2 and *mys* RNAi flies 9,84 (±0,174) µm2 (p=4,55×10^{-6}). The second area that showed statistical significance in cell size was 1st posterior area. In control flies cell size was 9,511(±0,284) µm^2 and *mys* RNAi flies 10,33 (±0,164) µm^2 (p=1,873×10^{9}). The

third area that showed statistical significance in cell size was 2nd posterior area. In control flies cell size was 9,23 (±0,222) µm^2 and *mys* RNAi flies 10,211 (±0,233) µm2 ($p=2{,}236\times10^{-12}$). The fourth area that showed statistical significance in cell size was 3rd posterior area. In control flies cell size was 9,103 (±0,2856) µm^2 and mys RNAi flies 9,524 (±0,201) µm^2 ($p=8{,}706\times10^{-5}$). The next area that showed statistical significance in cell size was 1st basal area. In control flies cell size was 7,88 (±1,036) µm^2 and *mys* RNAi flies 8,174 (±0,136) µm^2 ($p=2{,}46\times10^{-6}$). Checking the costal area there was also statistical significance detectable (p=0,038), but it is not part of wing blade area (Figure 18).

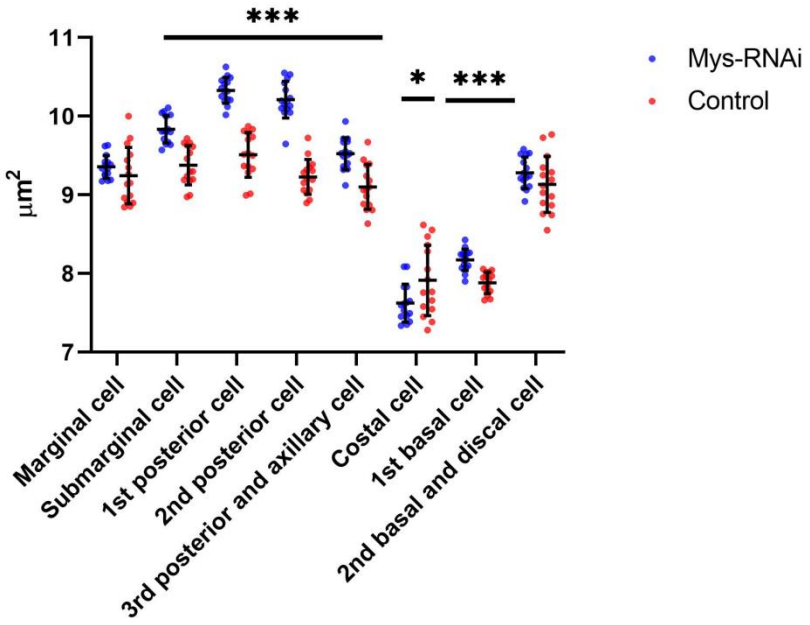

Figure 18. Average cell size of each intervein area at 16h BPF *mys* knock-out time. Evaluating the effect of *mys* to wing development is to find out whether disruption of mys expression causes any difference in intervein cell size. As a result, all intervein area cell were statistically different except marginal and 2nd basal and discal area. (*p≤0.05; **p≤0.01; ***p≤0.001)

Additionnaly, comparing trichomes between control and *mys* RNAi flies, were discovered that switching off gene *mys* at stage of starting at prepupa formation, caused defects in wing hair orientation. Most of these mis-orientated hairs situated on 3rd posterior area (Figure 19A and 19B). Hairs are oriented on different directions, they grow at an uneven density and from one cell several hairs grow out. Margin hairs have large difference in thickness and length.

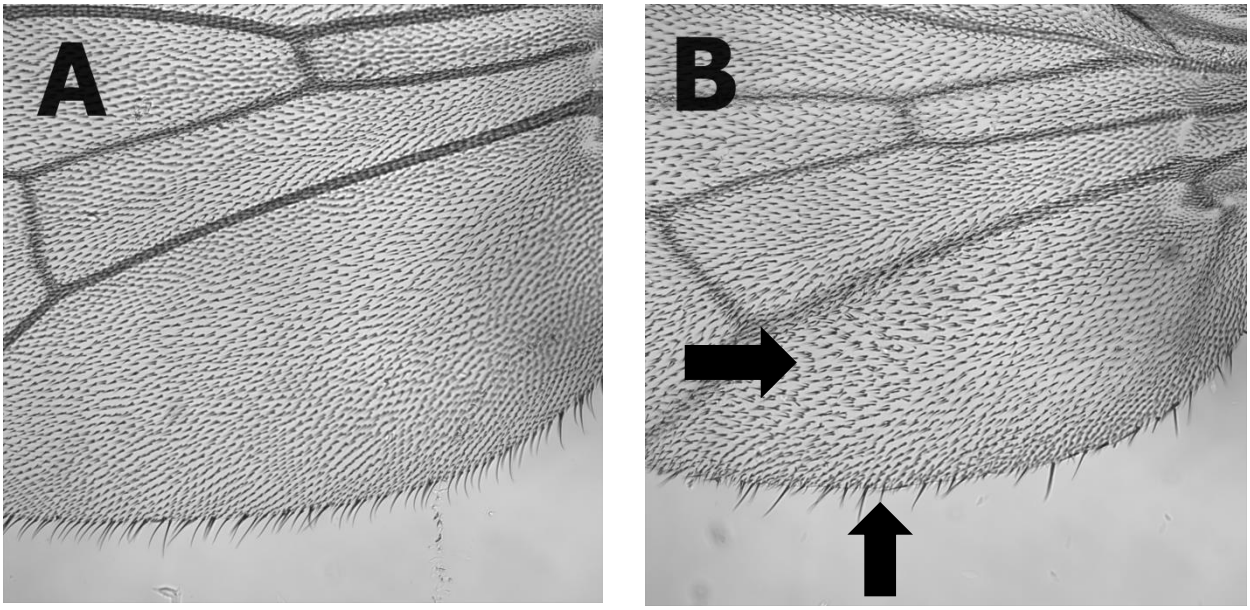

Figure 19. Abnormal wing hairs caused by mys deficiency. (A) In control flies wing hairs are orientated in parallel. (B) In mys RNAi flies one can see misorientation and unequal placement of wing hair (black arrows).

.

2.4. Discussion

According to the results of pilot screening, genotypes found in this process were mutants which reduced the adult wing size follow: UAS-*cdc42* DN, UAS-*rab9* RNAi; UAS-*mys* RNAi. Previously researched data shows that genes *cdc42*, *rab9* and *mys* are important in proliferation, thus inhibiting their expression leads to decreasing the tissue growth rate (Du *et al*., 2016; Li *et al*., 2019).

Analyzing more closely wing blade size one can see that the sooner *mys* expression is switched off in wing disc pouch during 3rd instar larva stage, the smaller wing blade will be gradually, but starting at the beginning of wing morphogenesis. According to Figure X, one can see a large gap in wing size starting at switching off the *mys* expression beginning of 16thh between control and *mys* RNAi group.

It is known that for instance, *dpp* is crucial for growth of Drosophila wing, but it has been observed that eliminating *dpp* expression from wing disc pouch area 24h BPF maintains normal rate of cell proliferation and exhibit mild defects in growth of wing imaginal disc (Akiyama and Gibson, 2015). According to Jinghua Giu, it is seen that *dpp* knock-out induced in the wing pouch area of its imaginal disc 24h BPF causes ablated *dpp* expression in pupal wings and also significantly smaller pupal wing in size 24h AP (Gui *et al*., 2019). It is also known that *mys* expression regulates positively Sog activity which is involved on the transport of *Dpp* (Araujo *et al*., 2003). Additionally, it is shown that collagen IV enhances Dpp signaling and promote the morphogen gradient formation during D/V patterning in the Drosophila embryo via integrin signaling (Ashe, 2016). Comparing previous information and data of this study, one may draw parallels between *mys* and *dpp* signaling. It is known that Dpp expressed in the longitudinal vein primordia cells diffuses laterally during pupal wing inflation stage which is important for normal proliferation. It can be hypothesis why cell density in intervein areas of adult wing of *mys* knock-out fly is smaller. Relataed to that, for the next step can be do for *dpp* and *mys* co-working could be checking the lateral migration of Dpp signal at different timepoints in *mys* deficient fly. Based on the results of this study, one can be concluded that β-integrin Myospheroid is an important protein for affecting general size, size majority of intervein segments, cell density and size of intervein areas of adult wing of *Drosophila melanogaster*.

Counting the trichomes of adult fly wing there was noticed that trichome positioning was misaligned or more than one hair can be grown out from one cell. This phenotype is common in planar cell polarization defects. It is known that loss of *mys* function cause defects in ommatidial rotation of *Drosophila melanogaster*. Frizzled/PCP factors, acting through RhoA and Rho kinase, regulate the function/activity of integrins and that integrins thereafter contribute to the complex interaction network of PCP signaling (Thuveson *et al*., 2019).

According to results may conclude that *mys* is important of attaching dorsal and ventral layer, it can be important playing a role on planar cell polarity. Epithelial polarity is established by multiple complexes, but Par, Crumbs and Scribble are coordinating events. Distinct membrane targeting and endocytic recycling pathways direct apical and basolateral proteins to the correct membrane surface. These mechanisms providing fully polarized epithelial cell. Epithelial orientation needs extrinsic signals which originate from ECM.

β1 integrins are widely expressed in epithelial cells and genetic deletion approaches have revealed that they have a central role in maintaining their polarity, as well as in other cell types, for instance endothelia. Integrins control both basement membrane deposition and intracellular apical–basal orientation. (Ojakian and Schwimmer, 1994; Wang *et al*., 1990).

Conclusion

The aim of the thesis was to find suitable protein among 23 different mutants of Rab, Rho and integrins for co-signalling with Dpp, affecting size of adult wing. As a result of pilot screening, there were found 6 different mutations in females that had an effect to Drosophila wing size. Female mutants were follow: ubi>αTubulin:GFP; *nubbin*-Gal4/UAS-*rab5* RNAi; tub-80ts/+ ; ubi>αTubulin:GFP; *nubbin*-Gal4/UAS-*rab8* CA; tub-80ts/+ ; ubi>αTubulin:GFP; *nubbin*-Gal4/UAS-*rab9* RNAi; tub-80ts/+ ; ubi>αTubulin:GFP; *nubbin*-Gal4/UAS-*rac1* RNAi; tub-80ts/+ ; ubi>αTubulin:GFP; *nubbin*-Gal4/UAS-mys RNAi; tub-80ts/+ ; ubi>αTubulin:GFP; *nubbin*-Gal4/UAS-scab RNAi; tub-80ts/+. Also 4 different mutations in male were found that affect wing size. Results were follow: ubi>Tubulin:GFP/y; *nubbin*-Gal4/UAS-*rab8* CA; tub-gal80ts/+ ; ubi>Tubulin:GFP/y; *nubbin*-Gal4/+; tub-gal80ts/UAS-*rac1* RNAi; ubi>αTubulin:GFP/y; *nubbin*-Gal4/UAS-*cdc42* DN; tub-gal80ts/+ ; ubi>Tubulin:GFP/y; *nubbin*-Gal4/UAS-*mys* RNAi; tub-gal80ts/+.

Concentrating on *mys* RNAi, one can conclude that there are many similarities according to Dpp deficient fly. Switching off the *mys* expression 24h BPF causes decreation in pupal wing size, but the size wing imaginal discs pouch area remained unchanged.

Also *mys* RNAi mutant causes diminishing the density of trichomes in most of intervein segments (submarginal area, 1st posterior area, 2nd posterior area, 3rd posterior area and 2nd basal and discal area), but average cell size in *mys* RNAi was larger.

One can conclude that gene *mys* RNAi causes changes in size of *Drosophila melanogaster* wing, but not imaginal disc wing pouch.

Resümee

ß-integriini *myospheroid* roll äädikakärbse *Drosophila melanogaster*-i tiiva arengus

Marko Leevik

Organismi funktsioneerimist on põhjalikult uuritud, kuid uued teadusavastused tekitavad üha rohkem uusi küsimusi. Teaduse tehnoloogia arenedes tehakse üha täpsemaid avastusi pealtnäha juba põhjalikult uuritud valdkondades.

Elusolendid koosnevad rakkudest. Integriinid, mis funktsioneerivad justkui rakkude "käed", olles primaarseteks retseptoriteks ekstratsellulaarsele maatriksile. Integriinid asuvad rakumembraanis ja vahendavad organismis mitmeid arengubioloogiliselt olulisi funktsioone ja signaaliradu. Üheks näiteks on evolutsiooniliselt konserveerunud signalisatsioonivalkude grupp *Bone Morphogenetic Protein* (BMP). BMP on kõrgelt konserveerunud mitmetes liikides. Näiteks on äädikakärbse *Drosophila melanogaster*-i BMP ekvivalendiks *Decapentaplegic* (Dpp), mis on inimese BMP2 ja BMP4 ortoloogid. BMP signaliseerimine on vajalik rakkude proliferatsiooniks, kudede suuruse reguleerimiseks ning rakkude diferentseerumiseks. Seega võib väita, et organism on pidevalt dünaamilises arengus.

Antud magistritöö eesmärgiks oli kirjeldada β-integriini *myospheroid* RNAi aegruumilist efekti epiteliaalsele morfogeneesile mudelorganismis *Drosophila melanogaster*, kasutades UAS/GAL4 süsteemi termosensitiivse GAL80 süsteemi kontrolli all. Kärbeste tiibu ja imaginaardiskide *pouch* piirkondi mõõdeti mitmel erineval ajapunktil alates 3. *instar larva* staadiumi teisest poolest ning leiti, et *mys* geeni väljalülitamine ei mõjuta imaginaardiski *pouch* piirkonna suurust, kuid vähendab täiskasvanud kärbeste tiiva ümbermõõtu ning samuti ka *pupa* tiiva ümbermõõtu, kellel on *mys* RNAi aktiveeritud. Samuti täheldati muutusi ka täiskasvanud isendi tiiva eri segmentide karvakeste/rakkude arvus, suuruses ja tiheduses, võrreldes mutantseid isendeid kontrollisenditega.

References

Adams, M.D., Celniker, S.E., Holt, R.A., Venter, J.C. (2000). The Genome Sequence of Drosophila melanogaster. Science 287, 2185-2195.

Affolter, M., K. Basler, K. (2007). The Decapentaplegic morphogen gradient: from pattern formation to growth regulation. Nat. Rev. Gen., 8, 663-674

Akiyama, T., Gibson, M. C. (2015). Decapentaplegic and growth control in the developing Drosophila wing. Nature 527 (7578), 375-378

Araujo, H., Negreiros, E., Bier E. (2003). Integrins modulate Sog activity in the Drosophila wing. Development 130, 3851-3864. doi: 10.1242/dev.00613

Ashe, H. L. (20016). Modulation of BMP signalling by integrins. Biochemical Society Transactions 44, 1465–1473 DOI: 10.1042/BST20160111

Johnson, A. B., J. (2002). Lewis, Molecular Biology of the Cell. 4th edition. New York: Garland Science; Integrins.

Aldaz, S., Escudero, L. M., Freeman, M. (2010). Live imaging of Drosophila imaginal disc development. Proc. Natl. Acad. Sci. 107(32): 14217–14222. doi:10.1073/pnas.1008623107

Arias, A. M. (2008). Drosophila melanogaster and the development of biology in the 20th century. Methods Mol Biol. 420, 1-25. doi: 10.1007/978-1-59745-583-1_1.

Bachmann, A. and Knust, E. (1998). Positive and negative control of Serrate expression during early development of the Drosophila wing. Mech Dev 76(1-2), 67-78.

Bainbridge, P., S. and Bownes, M. (1988). Ecdysteroid titers during Drosophila metamorphosis. Insect Biochemistry, 18(2), 185–197. doi:10.1016/0020-1790(88)90023-6

Basler, K. and Struhl, G. (1994). Compartment boundaries and the control of Drosophila limb pattern by hedgehog protein. Nature 368(6468), 208-214.

Bate, M. and Arias, A.M. (1991). The embryonic origin of imaginal discs in Drosophila. Development 112(3), 755-761.

Bejarano, F., Lidia Pérez, L., Apidianakis, Y., Delidakis, C., and Marco Milán, M. (2007). Hedgehog restricts its expression domain in the Drosophila wing. EMBO Rep. 8(8), 778–783. doi: 10.1038/sj.embor.7401003

Blair, S. S., Brower, D. L., Thomas, J. B., Zavortink, M. (1994). The role of apterous in the control of dorsoventral compartmentalization and PS integrin gene expression in the developing wing of Drosophila. Development, 120: 1805-1815, 1994.

Brabant, M. C., Fristrom, D., Bunch, T. A., and Brower, D. L. (1996). Distinct spatial and temporal functions for PS integrins during *Drosophila* wing morphogenesis. Development 122, 3307–3317.

Bridges, C. B. (1936). D.I.S. work sheet no. 1: external structure of Drosophila. Drosophila Information Service 6, 76.

Brower, D. L., Wilcox, M., Piovant, M., Smith, R. J., and Reger, L. A. (1984). Related cell-surface antigens expressed with positional specificity in Drosophila imaginal discs. Proc. Natl. Acad. Sci. USA 81, 7485–7489

Brown, N. H., Gregory, S. L., Martin-Bermundo, M. D. (2000). Integrins as Mediators of Morphogenesisin Drosophila. Developmental Biology 223, 1-16. doi:10.1006/dbio.2000.971

Cheresh, D. A., Mecham, R. P. (1994). "Integrins: Molecularand Biological Responses to the Extracellular Matrix." AcademicPress, London

Classen, A. K., Aigouy, B., Giangrande, A., Eaton S. Imaging Drosophila pupal wing morphogenesis. Methods Mol. Biol. 2008; 420, 265–275. doi: 10.1007/978-1-59745-583-1_16

Colombani, J., Andersen D.S, and Leopold, P. (2012). Secreted peptide Dilp8 coordinated Drosophila tissue growth with developmental timing. Science 336: 582-585. doi: 10.1126/science.1216689

Dahmann, C. and Basler, K. (1999). Compartment boundaries: at the edge of development. Trends Genet 15(8), 320-326.

Du, D-S., Yang, X-Z., Wang, Q., Dai, W-J., Kuai, W-X., Liu, Y-L., Chu, D., Tang, X-J. (2016). Effects of CDC42 on the proliferation and invasion of gastric cancer cells. Mol Med Rep (1):550-4. doi: 10.3892/mmr.2015.4523. Epub 2015 Nov 6.

Dye, N. A., Popović, M., Spannl, S., Etournay, R., Kainmüller, D., Ghosh, S., Myers, E. W., Jülicher, F., Eaton, S. (2017). Cell dynamics underlying oriented growth of the Drosophila wing imaginal disc. Development 144, 4406-4421. doi: 10.1242/dev.155069

Etournay, R., Merkel, M., Popović, M., Brandl, H., Dye, N. A., Aigouy, B., Salbreux, G., Eaton, S., Jülicher, F. (2016). TissueMiner: A multiscale analysis toolkit to quantify how cellular processes create tissue dynamics. eLife 5: e14334. DOI: 10.7554/eLife.14334

Fernández-Moreno, M. A., Farr, C. L., Kaguni, L. S., Garesse, R. (2007). Drosophila melanogaster as a Model System to Study Mitochondrial Biology. Methods Mol Biol. 2007 ; 372: 33–49. doi:10.1007/978-1-59745-365-3_3.

Festing, S., and Wilkinson, R. (2007). The ethics of animal research. Talking Point on the use of animals in scientific research. EMBO Rep. 2007 Jun; 8(6), 526–530. doi: 10.1038/sj.embor.7400993

Flagg, R.O. (1988). Carolina Drosophila Manual, p.8. Carolina Biological Supply Co

Fortini, M.E., Skupski, M.P., Boguski, M.S., and Hariharan, I.K. (2000). A Survey of Human Disease Gene Counterparts in the Drosophila Genome. J. Cell Biol. 150, 23F-30.

Friedman, R., Hughes, A. L. (2001). Pattern and Timing of Gene Duplication in Animal Genomes. Genome Res. 11, 1842-1847.

Fristrom, D. and Fristrom, J. (1992). The metamorphic development of the adult epidermis. In The Development of Drosophila (ed. A. Martinas Arias and M. Bates,). Cold Spring Harbor, New York: Cold Spring Harbor Press (in press)

Fristrom, D., Wilcox, M., Fristrom, J. (1993). The distribution of PS integrins, laminin A and F-actin during key stages in Drosophila wing development. Development 117: 509-523.

Fristrom, D., and Liebrich, W. (1986). The hormonal coordination of cuticulin deposition and morphogenesis in Drosophila imaginal discs in vivo and in vitro. Developmental Biology, 114(1): 1–11. doi:10.1016/0012-1606(86)90378-7

Gui, J., Huang, Y., Montanari, M., Toddie-Moore, D., Kikushima, K., Nix, S., Ishimoto, Y., Shimmi, O. (2019). Coupling between dynamic 3D tissue architecture and BMP morphogen

signaling during Drosophila wing morphogenesis. Proc. Natil. Acad. Sci. U.S.A 16(10) 4352–4361. doi:10.1073/pnas.1815427116

Haga, R. B., Ridley, A. J. (2016). Rho GTPases: Regulation and roles in cancer cell biology. SMALL GTPASES VOL. 7, NO. 4, 207–221 http://dx.doi.org/10.1080/21541248.2016.1232583

Hynes, R. O. (1992). Integrins: Versatility, modulation, and signal-ing in cell adhesion. Cell 69; 11–25

Kornberg, T., Siden, I., O'Farrell, P., and Simon, M. (1985). The *engrailed* locus of *Drosophila*: In situ localization of transcripts reveals compartment-specific expression. Cell 40, 45-53.

Liu, Y., Wang, X., Zhang, Z., Xiao, B., An, B., Zhang, J. (2019). The overexpression of Rab9 promotes tumor progression regulated by XBP1 in breast cancer. Onco Targets Ther. 12: 1815–1824. doi: 10.2147/OTT.S183748

Martin-Bermudo, M. D., Alvarez-Garcia, I., Brown, N. H. (1999). Migration of the Drosophila primordial midgut cells requires coordination of diverse PS integrin functions. Develop-ment 126,5161–5169.

Michel, M., Aliee, M., Rudolf, K., Bialas, L., Jülicher, F., Dahmann, C. (2016). The Selector Gene apterous and Notch Are Required to Locally Increase Mechanical Cell Bond Tension at the Drosophila Dorsoventral Compartment Boundary. PLoS One. 11(8); e0161668. doi: 10.1371/journal.pone.0161668

Milan, M., Campuzano, S., Garcia-Bellido, A. (1996). Cell cycling and patterned cell proliferation in the Drosophila wing during metamorphosis. Proc. Natl. Acad. Sci. U.S.A. 93(21): 11687-11692. 10.1073/pnas.93.21.11687

Mitchell, H. K., Edens, J. and Petersen, N. S. (1990). Stages of cell hairconstruction in Drosophila. Dev. Genetics 11, 133-140. doi: 10.1002/dvg.1020110203.

Mitchell, H. K., Roach, J. and Petersen, N. S. (1983). The morphogenesis of cell hairs on Drosophila wings. Dev. Biol. 95, 387-398. doi.org/10.1016/0012-1606(83)90040-4

Murray M. A., Schubiger, M., Palka, J. (1984). Neuron differentiation and axon growth in the developing wing of Drosophila melanogaster. Dev. Biol. 104: 259-273. doi.org/10.1016/0012-1606(84)90082-4

McBrayer, Z., Ono, H., Shimell, M., Parvy, J.-P., Beckstead, R. B., Warren, J. T., … O'Connor, M. B. (2007). Prothoracicotropic Hormone Regulates Developmental Timing and Body Size in Drosophila. Developmental Cell, 13(6): 857–871. doi:10.1016/j.devcel.2007.11.003

Narashima M, Brown NH. (2000-2013). Integrins and Associated Proteins in Drosophila Development. In: Madame Curie Bioscience Database [Internet]. Austin (TX): Landes Bioscience

Neto-Silva, R. M., Wells, B. S., Johnston, L. A. (2009). Mechanisms of growth and homeostasis in the Drosophila wing. Annu Rev Cell Dev Biol. 25, 197–220. doi: 10.1146/annurev.cellbio.24.110707.175242

Piddini, E. and Vincent, J.P. (2009). Interpretation of the wingless gradient requires signalinginduced self-inhibition. Cell 136(2), 296-307.

Schubiger, M., and Palka, J. (1987). Changing spatial patterns of DNA replication in the developing wing of Drosophila. Devel. Biol. 123, 145—153

Schwartz, S. L., Cao, C., Pylypenko, Rak, A., Wandinger-Ness, A. (2007). Rab GTPases at a glance. Journal of Cell Science 2007 120: 3905-3910; doi: 10.1242/jcs.015909

Journal of Cell Science 2007 120: 3905-3910; doi: 10.1242/jcs.015909

St Johnston, D. (2002). The art and design of genetic screens: Drosophila melanogaster. Nature Reviews Genetics 3, 176-188.

Stark, K. A., Yee, G. H., Roote, C. E., Williams, E. L., Zusman, S.,and Hynes, R. O. (1997). A novelaintegrin subunit associates with βPS and functions in tissue morphogenesis and movementduringDrosophiladevelopment.Development 124,4583– 4594.

Streuli, C. H. (2009). Integrins and cell-fate determination. Journal of Cell Science 122, 171-177. doi:10.1242/jcs.018945

Thuveson, M., Gaengel, K., Gollu, G. M., Chin, M. I., Singh, J., Mlodzik, M. (2019). Integrins are required for synchronous ommatidial rotation in the Drosophila eye linking planar cell polarity signalling to the extracellular matrix. The Royal Society Publishing. https://doi.org/10.1098/rsob.190148

Tyler, M. S. (2000). Developmental Biology, A Guide for Experimental Study, p. 1-11. Second Edition, Sinauer Associates, Inc. Publishers, Sunderland, MA., ISBN 0-87893-843-5

Waddington CH (1940) The genetic control of wing development in Drosophila. J Genet 41: 75-139.

Wang, S-H., Simcox, A., Campbell, G. (2000). Dual role for Drosophila epidermal growth factor receptor signaling in early wing disc development. Genes Dev. 14(18), 2271–2276. doi: 10.1101/gad.827000

Wilcox, M., Brown, N., Piovant, M., Smith, R. J., and White, R. A.(1984). The *Drosophila* position-specific antigens are a family of cell surface glycoprotein complexes.EMBO J.3,2307–2313. doi.org/10.1002/j.1460-2075.1984.tb02131.x

Wright, T. R. F. (1960). The phenogenetics of the embryonicmutant, lethal myospheroid, in *Drosophila melanogaster*. J. Exp.Zool.143, 77–99. doi.org/10.1002/jez.1401430107

Zecca, M., Struhl, G. (2002). Control of growth and patterning of the Drosophila wing imaginal disc by EGFR-mediated signaling. Development 129, 1369-1376

Zecca, M., Struhl, G. (2002). Subdivision of the Drosophila wing imaginal disc by EGFR-mediated signaling. Development 129, 1357-1368;

Zecca, M., Basler, K., Struhl, G. (1995). Sequential organizing activities of engrailed, hedgehog and decapentaplegic in the Drosophila wing. Development 121(8), 2265-2278.

Materials from webpage

http://flymove.uni-muenster.de/Genetics/Flies/LifeCycle/LifeCyclePict/life_cycle.jpg

https://www.uniprot.org/uniprot/P11584

Non-exclusive licence to reproduce thesis and make thesis public

I, Marko Leevik
(*author's name*)

1. herewith grant the University of Tartu a free permit (non-exclusive licence) to

reproduce, for the purpose of preservation, including for adding to the DSpace digital archives until the expiry of the term of copyright,

The role of β-integrin *myospheroid* in the wing development of *Drosophila melanogaster*,
(*title of thesis*)

supervised by professor Osamu Shimmi and PhD Tambet Tõnissoo.
(*supervisor's name*)

2. I grant the University of Tartu a permit to make the work specified in p. 1 available to the public via the web environment of the University of Tartu, including via the DSpace digital archives, under the Creative Commons licence CC BY NC ND 3.0, which allows, by giving appropriate credit to the author, to reproduce, distribute the work and communicate it to the public, and prohibits the creation of derivative works and any commercial use of the work until the expiry of the term of copyright.

3. I am aware of the fact that the author retains the rights specified in p. 1 and 2.

4. I certify that granting the non-exclusive licence does not infringe other persons' intellectual property rights or rights arising from the personal data protection legislation.

Marko Leevik
12/08/2020